Master's thesis

Phase transitions between fractional quantum Hall states: a Bose condensation approach

Shanna M. Haaker

Supervisor: Prof. dr. F.A. Bais

August 4, 2009

Universiteit van Amsterdam

Abstract

The work we describe in this thesis is inspired by the recent developments towards an intrinsically fault-tolerant form of quantum computation to be implemented in physical systems that exhibit topologically ordered phases. We investigate transitions between different topological phases by condensation of bosonic quasiparticles. This provides us with a full description of the excitations in the bulk of these phases as well as on the domain wall separating them. We apply this method to several fractional quantum Hall states. Included is a phase transition between the MR and NASS state where the wall between these phases turns out to have the same order as a minimal model at central charge $c = 7/10$. Both the MR and NASS state carry anyons with non-Abelian statistics making them suitable for doing quantum computations. The different quantum numbers carried by these quasiparticles are obtained and processes that involve particles from both regions and the wall are discussed. Furthermore, we successfully obtain spectra for fractional quantum Hall states belonging to the Haldane-Halperin and Bonderson-Slingerland hierarchies. The former describes Abelian Hall states in the lowest Landau level and the latter non-Abelian ones in the second Landau level, including the MR state at $\nu = 5/2$. Especially, we focus on the domain wall between different phases of the same hierarchy, where we obtain electric charges of the fundamental excitations on these walls.

Contents

CHAPTER 1

Introduction

Over the past decades, there has been a growing interest in studying topological phases of matter. With the discovery of fractional quantum Hall (FQH) fluids, which are systems that are expected to exhibit such topological phases, we have real physical systems at hand to test the theory. These fluids are believed to have anyonic excitations which in some cases could be of the non-Abelian type. The different states such non-Abelian particles can be in, lead to a natural way of storing quantum information. This opens the door to building fault tolerant quantum computers, which is an important application and therefore, makes them extremely interesting not only for physicists.

With this application in the back of our minds, it is necessary to enlarge our knowledge of topological phases and in particular of FQH states. The starting point for our work is that we are able to characterize a given topologically ordered phase by some algebraic structure, a quantum group or Hopf algebra. In this thesis we go a step further and analyse transitions between different topological phases induced by a condensate of bosonic degrees of freedom. In other words, we will develop the notion of the breaking of quantumsymmetries. The phases that are discussed in this thesis are all FQH states. This method has been successfully applied in earlier work and is complementary to the more conventional way to deal with FQH systems in terms of wavefunctions. We look directly at the underlying symmetry of

these states. In practice, this means that the topological excitations are labeled by representations of a quantum group corresponding to the symmetry of the system. These excitations carry certain quantum numbers associated to their statistics and fusion rules. When there is a bosonic particle present in the theory it can form a condensate, which breaks the symmetry of the initial spectrum. This might induce a transition to a new topological phase. It turns out that this approach automatically provides us with a description not only of the spectrum of the initial and final phase, but also of the domain wall between them.

The different chapters of this thesis roughly fall into two parts. First, chapter 2 and 3 present some of the theory behind the physics of topological phases. Second, chapter 4 and 5 apply the theory to some specific physical systems.

We start in chapter 2 with setting the stage of $(2+1)$-dimensional physics. A quick introduction on planar quantum statistics is given, which results in the notion of anyons; particles that are neither bosons nor fermions. Two quantum numbers are introduced that are carried by anyons: topological spin and quantum dimension, associated to rotating anyons and fusing them respectively. We end the first section by illustrating all these concepts using the Fibonacci model. The next section gives a review of the quantum Hall effect and states that have been proposed in the literature to describe the physics at the Hall plateaus. Also, experiments that try to determine the charge and statistics of the excitations in a Hall fluid will be discussed. Chapter 2 ends with a section on how non-Abelian anyons can be used to encode qubits for a quantum computer. Again, the Fibonacci model, which has a non-Abelian anyon, serves as an example.

Chapter 3 presents the method we use to describe transitions between different topological phases. We start with a short section on quantum groups which label the excitations of a topological phase. After that, we present all the different steps of topological symmetry breaking in section 3.2. These include identifying bosons in 2D, breaking the symmetry, finding the spectrum after a phase transition occurred, and determining what happens on the domain wall between two different phases. These concepts are put into practice using Kitaev's honeycomb model as an example.

This brings us to the second part of this thesis where topological symmetry breaking is applied to some explicit FQH states. Chapter 4 deals with a phase transition between a spin polarized state and a spin-singlet state, which are the so-called Moore-Read and NASS state respectively, where both carry non-Abelian anyons. We analyze the spectrum of the phases as well as of the domain wall between them. Also, we discuss what happens when a quasihole is dragged from one phase to the other and how qubits

can relax their internal state. Both processes include the domain wall in a non-trivial way.

Chapter 5 presents how the same method can be applied to the hierarchy picture of the FQH effect. This picture, of building different Hall states on top of each other, will be explained in section 5.1. We explicitly derive the excitation spectra of two different hierarchy pictures, where one is Abelian and the other non-Abelian. Starting with two specific examples in section 5.2 we will present general formulae in section 5.3 of the excitation spectra and the associated quantum numbers.

Finally, in chapter 6, the main results will be summarized and we present an outlook for interesting future research.

CHAPTER 2

Features of planar physics

This thesis is concerned with topological phases of matter. We investigate such phases and their spectra by means of topological symmetry breaking. Before we reach this point we should set the stage for topological phases; that is what this chapter is concerned with.

In section 2.1 we start by considering the problem of quantum statistics of particles in two dimensions and contrast it with the situation in three dimensions. In three dimensions particles have either bosonic or fermionic statistics corresponding to completely symmetric or antisymmetric multiparticle states. However, in two dimensions the conditions for consistency are far less restrictive opening up novel possibilities denoted as fractional spin and braid statistics. These exotic properties are a key element to understanding the physics of anyons; the typical excitations that exist in topologically ordered phases.

Section 2.2 gives a brief introduction to Quantum Hall fluids. These are topological phases which are being observed in the laboratory. The observed characteristics of these fluids are discussed, as well as the theory that tries to describe the observations. Also, some experiments on how to determine the quantum numbers of the particles in FQH fluids will be discussed.

The present chapter ends with a section on topological quantum compu-

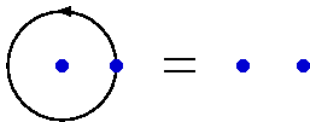

Figure 2.1: *Quantum statistics of two identical particles in three or more spatial dimensions. Taking a particle around the other is topologically equivalent to doing nothing at all.*

tation (TQC), which opens the door to fault-tolerant quantum computers and can be viewed as the application that inspired physicists to seriously investigate topological order.

To keep the theory of this chapter as transparent as possible we will use the Fibonacci model as a theoretical discourse in this chapter.

2.1 Quantum statistics in planar physics

This section will closely follow the lines of Ref. [1, 2]. Before considering systems in two spatial dimensions, let us first go one dimension up. When we have a system of two identical particles and they are interchanged twice, this operation is identical to bringing one particle around the other, in such a way that their final positions coincide with the initial positions. The trajectory of the particle that was taken around the other can be smoothly deformed and shrunk to a single point, which is shown in Fig. 2.1. These situations are topologically equivalent. This result has to be incorporated in the wave function describing the system. It has to pick up a phase factor of either $+1$ or -1 when two particles switch positions. The $+1$ corresponds to particles with Bose statistics and -1 to particles with Fermi statistics.

After this rather brief review of statistics in 3-dimensional systems where there naturally arise two types of particles, namely bosons and fermions,

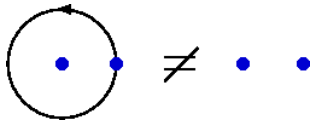

Figure 2.2: *Quantum statistics of two identical particles in two spatial dimensions. Taking a particle around the other results in a non-trivial operation acting on the wave function of the system.*

we turn to our case of interest. Fig. 2.2 shows the difference in statistics between two dimensions and the 3-dimensional case. This time we cannot smoothly deform the trajectory of the particle that has been taken around the other, since we would have to cut through the other particle.

For three spatial dimensions particles fall into two classes: bosons and fermions, which followed from the invariance under interchanging particles twice. For two dimensions this no longer holds and we must find a way of describing the different ways in which these particles can be interchanged in planar systems. This will be explained in the following.

2.1.1 Braid group

The statistics of N identical particles in two spatial dimensions is governed by the *braid group*, $\mathcal{B}_N$. Let us start with a comment on the name of this group. When considering (2+1)-dimensional physics we can keep track of the spacetime coordinates of an object by drawing its trajectory. For a point particle these are lines, which in this context are called *worldlines*. When an element of the braid group acts on the particles it interchanges them, i.e. it braids their worldlines.

Clearly, the braid group is an infinite group, since we can just keep on interchanging the particles. Still, it is generated by a finite number of generators. For N particles there must be $N-1$ generators, denoted by σ_i. As an example consider a system with three indistinguishable particles. The action of the two generators of the braid group are shown in Fig. 2.3. The σ_1 generator exchanges the leftmost particle with its neighbor in a counter-clockwise way. The σ_2 generator does the same for the second particle and its neighbor to the right. Their inverses execute the same action, but in a clockwise way.

The generators for N particles satisfy the following, defining relations

$$\begin{array}{lcll} \sigma_i\sigma_j & = & \sigma_j\sigma_i & \text{for} \quad |i-j| \geq 2 \\ \sigma_i\sigma_{i+1}\sigma_i & = & \sigma_{i+1}\sigma_i\sigma_{i+1} & \text{for} \quad \forall i \end{array} \tag{2.1}$$

The last of these is called the Yang-Baxter equation and it is graphically shown in Fig. 2.4. Since a clockwise and a counter-clockwise exchange of particles is not the same (see Fig. 2.4), we have

$$\sigma_i^2 \neq 1 \tag{2.2}$$

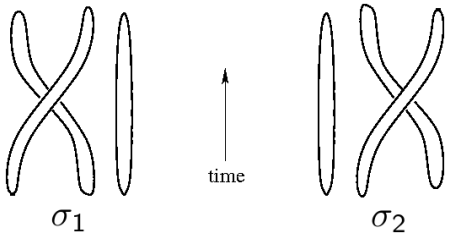

Figure 2.3: *The action of the two generators of the braid group corresponding to a system with three identical particles. The worldlines of the particles are shown.*

The fact that the square of a generator is not equal to unity makes the braid group so different from the permutation group (which deals with exchanging identical particles in 3- or higher-dimensional physics).

After presenting the main features of the braid group the next subsection shows how the braid group can label the particles that arise in 2-dimensional physics.

2.1.2 Anyons

Let us, again for a moment, return to a 3-dimensional system with N indistinguishable particles. In this case an action of the permutation group $\mathcal{S}_N$ on the system results in interchanging the particles. The permutation group has two 1-dimensional irreducible representations and it is exactly those two irreps that label bosons and fermions.

In the same way we use the irreps of the braid group to label particles in 2-dimensional systems. The 1-dimensional irreps of the braid group are just the phases that the quantum state of the system picks up when particles are exchanged. For a wavefunction $\psi(r_1, r_2)$ describing two particles at coordinates r_1 and r_2 such an exchange results in

$$\Psi(r_1, r_2) \to e^{i\theta}\Psi(r_1, r_2) \tag{2.3}$$

Note that the fermionic and bosonic cases are also included in this phase factor; for two fermions we have $\theta = \pi$ and for bosons $\theta = 0$. Any other phase corresponds to particles called *anyons*. For the specific case in (2.3) it does not matter in which order the particles are braided, since the phase factors commute. We say that they are anyons with Abelian statistics, or

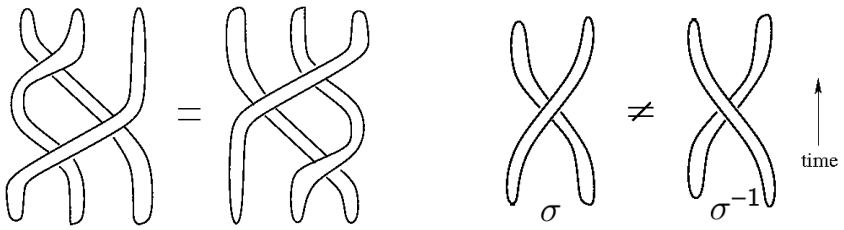

Figure 2.4: *Yang-Baxter equation for generators of the braid group is shown in the left figure. At the right it is displayed that, in general, a clockwise exchange of two particles is not the same as a counter-clockwise exchange.*

just Abelian anyons. But the braid group also has higher-dimensional irreps. In this case the wavefunction is a vector and the action of the braid group on the system is represented by matrix multiplication. Physically it means that there has to be a number of anyons at fixed positions which results in a degeneracy of the ground state. Exchanging particles mixes the different components of the wave function. This can be written as

$$\psi_\alpha \to [M(\sigma_i)]_{\alpha\beta}\psi_\beta \tag{2.4}$$

for some matrix representation $[M(\sigma_i)]$ of the braid group generators σ_i. In general matrices do not commute, which leads to the implication that for higher-dimensional irreps the order in which particles are braided does matter. The particles obey non-Abelian braiding statistics, i.e. they are non-Abelian anyons.

We have seen that when a system is in a *topological phase* its excitations are anyons. A more precise definition of such phases is that they are systems in which all observable properties are invariant under smooth deformations of the spacetime manifold, at long wavelengths, low temperatures and energies. In general, topological phases have a non-zero energy gap that separates the ground states from the excited states. Then, the only way that such a system can undergo a transformation is by braiding the anyons. This is exactly what happens in (2.4).

2.1.3 Fusion rules

Besides braiding there is another type of interaction between anyons. This is fusion of anyons. Imagine two anyons coming close together, at a certain point we cannot distinguish between them anymore. We could say that their

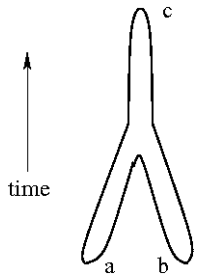

Figure 2.5: *Two anyons with topological charge a and b fuse to form an anyon with charge c.*

quantum numbers combine, i.e. they fuse to form a different particle (see Fig. 2.5). Consider a particle carrying some topological charge a and one with charge b, when they fuse, this can be written as

$$a \times b = \sum_c N_{ab}^c c \tag{2.5}$$

where N_{ab}^c is a positive integer that denotes the number of independent ways in which a and b can fuse to form c. For $\sum_c N_{ab}^c \geq 2$ they are non-Abelian anyons. These fusion rules are restricted by the following physical arguments:

Associativity $(a \times b) \times c = a \times (b \times c)$: When fusing three or more particles the order in which they are fused should not matter. The final outcome has to be the same.

Unique vacuum $a \times 1 = 1 \times a = a$: There has to be a charge denoted by 1 which will be called the vacuum charge, with the property that any anyon that is fused with it results in the same anyon.

Charge conjugate $a \times \bar{a} = 1 + \sum_{c \neq 1} N_{a\bar{a}}^c c$: Every anyon has its unique conjugate particle. When they fuse the vacuum should appear as a fusion channel, with $N_{a\bar{a}}^1 = 1$.

So far, no explicit quantum numbers, carried by the anyons, have been mentioned. The first one that needs to be addressed is the *quantum dimension* of an anyon. Formally this number is found by fusing an anyon a many times with itself. The asymptotic number of available fusion channels is $(d_a)^N$ where d_a is the quantum dimension of a. In practice, we will be using the following relation between fusion and quantum dimensions

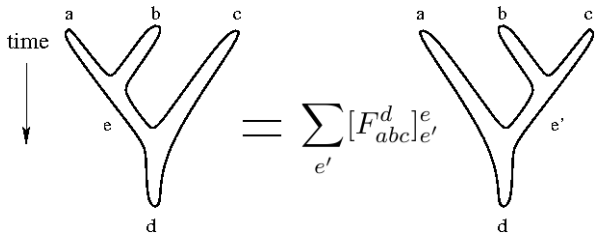

Figure 2.6: *The order in which anyons are fused does not change the final charge. This leads to different bases for the same Hilbert space. A change of basis is governed by the F-matrix.*

$$a \times b = \sum_c N^c_{ab} c \quad \Leftrightarrow \quad d_a d_b = \sum_c N^c_{ab} d_c \tag{2.6}$$

The associativity of the fusion rules implies that there are different bases for the same Hilbert space. Let us be more explicit on this. When three charges a, b and c fuse to form total charge d, it can happen in two ways. First a and b fuse to some intermediate charge e which then fuses with c to d, or b and c fuse to e' which fuses with a to d. If we denote the Hilbert space that is spanned by this fusion product by V^d_{abc} it can be decomposed into

$$V^d_{abc} \cong \bigoplus_e V^e_{ab} \otimes V^d_{ec} \cong \bigoplus_{e'} V^d_{ae'} \otimes V^{e'}_{bc} \tag{2.7}$$

This means that there are two bases for this Hilbert space. It may be useful to switch between those bases. The unitary transformation that performs this switch of bases is called the *F-matrix*. If we first fuse a and b to some intermediate charge e and then fuse it with c to form d this can be expressed in a different basis as (also see Fig. 2.6)

$$|((a \times b)_e \times c)_d\rangle = \sum_{e'} [F^d_{abc}]^e_{e'} |(a \times (b \times c)_{e'})_d\rangle \tag{2.8}$$

Whenever four particles are fused, we get more than two different bases. The F-matrix is restricted by the *pentagon relation* associated to this [3]. This relation is shown in Fig. 2.7 and it shows the associativity of four particles being fused to a fifth one.

If we want to change bases from $|(((1 \times 2)_a \times 3)_b \times 4)_5\rangle$ to one that has

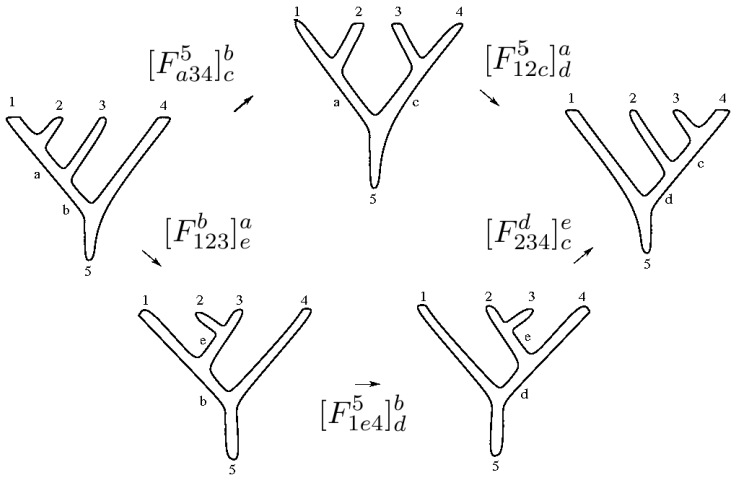

Figure 2.7: *Pentagon relation is imposed on the F-matrix. Moving through the upper part of the figure should always have the same final result as when taking the lower route.*

$|(1 \times (2 \times (3 \times 4)_c)_d)_5\rangle$ this can be done in two different ways represented by taking the upper path in Fig. 2.7 or the lower one. Both should give the same result, which leads to the pentagon equation:

$$[F^5_{12c}]^a_d [F^5_{a34}]^b_c = \sum_e [F^d_{234}]^e_c [F^5_{1e4}]^b_d [F^b_{123}]^a_e \tag{2.9}$$

which puts a restriction on the F-matrix. Moreover, one should note that these equations are also restricted by the specific fusion rules of the theory. In general, there are only a few solutions to these equations. At the end of the next subsection we will see another consistency relation that needs to be imposed on the theory which, together with the fusion rules and pentagon equations, fully determines an anyonic model. But first another quantum number associated to anyons will be introduced.

2.1.4 Spin factor

Let us consider the effect on the wave function of an anyonic system when a particle is rotated over a 2π angle. This results in a phase factor multiplying the initial wave function of the form

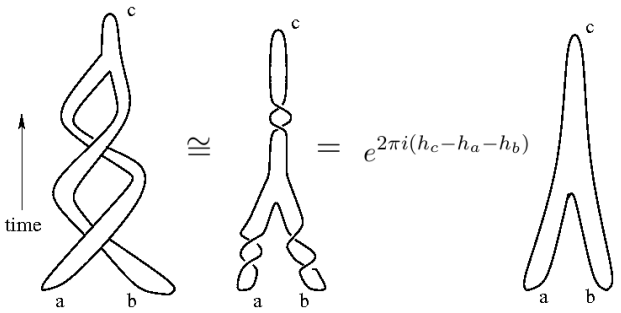

Figure 2.8: *The monodromy of particles a and b that are in fusion channel c is equal to rotating those particles over a 2π angle. This relates fusion to braiding.*

$$\theta_a = e^{2\pi i h_a} \tag{2.10}$$

We call this phase the *spin factor* of a and h_a, which appears in the exponent, the *topological spin* of a.[1] For a theory with a finite number of sectors, these spins are always rational [4].

The spin of an anyon can be used to relate braiding to fusion. In order to see this, first look at the *monodromy* of anyons. The monodromy of two particles is taking one particle around the other and then fusing them. This is visualized in Fig. 2.8 where it appears on the left hand side. Monodromy is topologicallly equivalent to counter-clockwise rotating both a and b over an angle of 2π and rotating their fusion channel c clockwise. This operation is shown in the second figure. Then (2.10) tells us that this is equal to just fusing the anyons and multiplying by a phase factor $e^{2\pi i(h_c-h_a-h_b)}$.

There is a more formal way to describe braiding of particles. This is by using the braid operator R, which is a map from the Hilbert space where a and b are fused to c, to one where the positions in space of a and b have been interchanged.

$$R : V_{ab}^c \to V_{ba}^c \tag{2.11}$$

This operation can also be expressed as a unitary matrix, which is called the *R-matrix*. Swapping the position of two particles leads to

[1] That it must be of the form (2.10) comes from the fact that h_a labels the representations of the covering group of the 2-dimensional rotation group, i.e. $U(1)$.

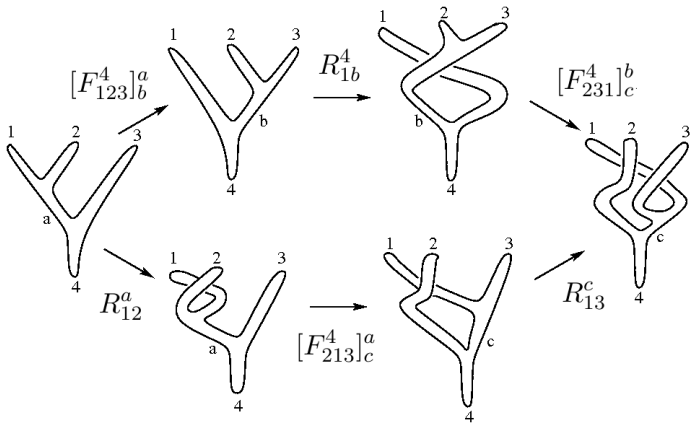

Figure 2.9: *The hexagon relation constrains the R- and F-matrices. Taking the upper path of this figure should have the same result as the lower one.*

$$(a \times b)_c = R^c_{ab}(b \times a)_c \tag{2.12}$$

In this notation the order in which the anyons appear is the same as their positions in space. As has been said before, besides the pentagon relation there is a second condition that can be imposed on the anyonic system. This is visualized in Fig. 2.9 and is called the *hexagon relation*. It combines changing bases with swapping particles which means that it puts constraints on the R- and F-matrix simultaneously. The hexagon equation can be written as

$$R^c_{13}[F^4_{213}]^a_c R^a_{12} = \sum_b [F^4_{231}]^b_c R^4_{1b}[F^4_{123}]^a_b \tag{2.13}$$

It turns out that the hexagon and pentagon conditions are the only ones that need to be met to ensure consistent braiding and fusing [2]. So if one has an anyonic model with a set of labels and its fusion rules and there exists solutions to the hexagon and pentagon equations then the model has the right physical properties.

Fusion and spin will be the main ingredients for topological symmetry breaking to be discussed in chapter 3. We will not be proving that knowing the fusion rules and spins of a topological phase fully pins down the corresponding TQFT. Still, for the examples we will be discussing we have not found two inequivalent TQFT's that have the same fusion rules and spins.[2]

[2]For an example of theories with the same fusion rules, but different spins look at the

2.1.5 Example: Fibonacci anyons

It seems helpful to go through what has been presented so far by using an explicit example. The model we choose for this is the Fibonacci model and it is fairly simple, but exhibits all of the structure that has been presented up until now. In this model there is only one non-trivial anyon denoted by τ and it is often called the Fibonacci anyon. The fusion rules are

$$1 \times 1 = 1 \qquad 1 \times \tau = \tau \times 1 = \tau \qquad \tau \times \tau = 1 + \tau \tag{2.14}$$

The fusion coefficients follow directly from this: $N_{11}^1 = N_{1\tau}^\tau = N_{\tau 1}^\tau = N_{\tau\tau}^1 = N_{\tau\tau}^\tau = 1$, the others are zero. Furthermore, we notice that τ is its own anti-particle. The fusion rule of τ with itself tells us that the Fibonacci anyon has to be a non-Abelian particle, since $\sum_i N_{\tau\tau}^i = 2$.

To find the quantum dimension of τ we simply consult relation (2.6), which leads to a set of equations

$$(d_1)^2 = d_1 \tag{2.15}$$
$$d_1 d_\tau = d_\tau \tag{2.16}$$
$$(d_\tau)^2 = d_1 + d_\tau \tag{2.17}$$

The first two equations independently set $d_1 = 1$, which results in $(d_\tau)^2 = 1 + d_\tau$. The outcome of this is the golden mean

$$d_\tau = \frac{1 + \sqrt{5}}{2} \tag{2.18}$$

The quantum dimension of the Fibonacci anyon could also have been deduced from the more formal definition. To this end, let us consider the dimension of the Hilbert space of n Fibonacci anyons, that ultimately fuse to the vacuum, $V_{\tau^n}^1$. The different independent ways in which this fusion product occurs can be expressed in terms of a *Bratelli diagram*. The different paths that can be taken gives the dimension of the Hilbert space. Such

Ising model. The fusion rules can be found in Tab. 4.1 as well as the spins of the Ising fields. This model is one out of eight inequivalent TQFT's that have the same fusion rules. They are $Ising, SU(2)_2, SO(5)_1, SO(7)_1$ and their complex conjugates. The fields of these theories that have the same fusion rules as σ, all have spins that differ from each other. This means that these theories have the same solution of the pentagon equation, but a different solution of the hexagon equation.

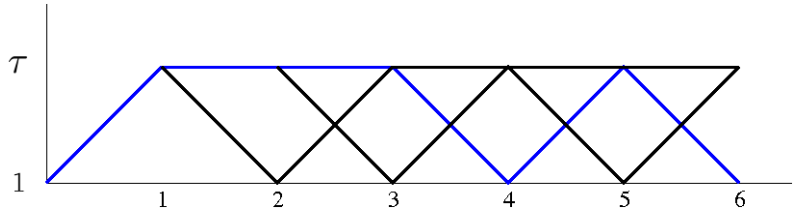

Figure 2.10: *Bratelli diagram for Fibonacci anyons. The dimension of the Hilbert space of n anyons of total charge $i = 1, \tau$ can be determined by counting the number of paths that lead to this charge. This diagram shows the possible paths for $n = 6$ anyons. One particular path with total charge $i = 1$ has been drawn in blue.*

a diagram is shown in Fig. 2.10. This leads to a recursion relation for the dimension of the Hilbert space, $D^1_{\tau^n}$:

$$D^1_{\tau^n} = D^1_{\tau^{n-1}} + D^1_{\tau^{n-2}} \tag{2.19}$$

Knowing that $D^1_{\tau^1} = 0$ and $D^1_{\tau^2} = 1$ this relation can be solved and leads to the Fibonacci numbers. It is known that these grow like

$$D^1_{\tau^n} \propto \phi^n \tag{2.20}$$

where $\phi \equiv \frac{1+\sqrt{5}}{2}$. This agrees with what we found before.

Let us now address the F-matrices. When fusing three anyons the total charge can either be 1 or τ, so we must find two F-matrices. Starting with the easiest one we can just invoke a change of bases

$$|(\tau \times (\tau \times \tau)_i)_1\rangle = \sum_j [F^1_{\tau\tau\tau}]^i_j |((\tau \times \tau)_j \times \tau)_1\rangle \tag{2.21}$$

Since the total charge has to be 1 it is easy to see that there is only one non-zero element:

$$[F^1_{\tau\tau\tau}] = \begin{pmatrix} 0 & 0 \\ 0 & 1 \end{pmatrix} \tag{2.22}$$

The pentagon relation is needed as well as unitarity to find the other F-matrix, $[F^{\tau}_{\tau\tau\tau}]$. Here we will only state the general solution:

$$[F^{\tau}_{\tau\tau\tau}] = \begin{pmatrix} \phi^{-1} & e^{i\theta}\sqrt{\phi^{-1}} \\ e^{-i\theta}\sqrt{\phi^{-1}} & \phi^{-1} \end{pmatrix} \tag{2.23}$$

where the phase factor that appears can be set to 1. Next, the hexagon relation (2.13) can be used to find the R-matrix. The only non-trivial case is where two Fibonacci anyons are fused to form either 1 or τ, $R^1_{\tau\tau}$ and $R^{\tau}_{\tau\tau}$ respectively. Since R needs to be a unitary matrix they can be written as $R^1_{\tau\tau} = e^{i\theta_1}$ and $R^{\tau}_{\tau\tau} = e^{i\theta_\tau}$. Plugging this into the hexagon equation together with (2.23) leads to

$$R^1_{\tau\tau} = e^{-4\pi i/5} \tag{2.24}$$
$$R^{\tau}_{\tau\tau} = -e^{-2\pi i/5} \tag{2.25}$$

Before we continue with determining all the possible ways in which a system of Fibonacci anyons can be manipulated, let us first consider the topological spin of an anyon. For this the monodromy of two such anyons will be used. Remember that this was interchanging two particles twice, i.e. R^2. On the other hand monodromy was also related to fusion by a phase factor which was shown in Fig. 2.8. This leads to

$$(R^{\tau}_{\tau\tau})^2 = e^{-4\pi i/5} = e^{-2\pi i h_\tau} \tag{2.26}$$

where the last equality must be met, from which it follows that the spin of the Fibonacci anyon is $h_\tau = 2/5$.

Knowing the R- and F-matrices we can in principle construct unitary matrices for any braid in a system of n Fibonacci anyons. For 3 particles this is still fairly simple, since there are only two generators of the braid group and the Hilbert space is 3-dimensional. The two matrices representing the generators are

$$\rho(\sigma_1) = \begin{pmatrix} e^{-4\pi i/5} & 0 & 0 \\ 0 & -e^{-2\pi i/5} & 0 \\ 0 & 0 & -e^{-2\pi i/5} \end{pmatrix} \tag{2.27}$$

$$\rho(\sigma_2) = \begin{pmatrix} -e^{-\pi i/5}\phi^{-1} & -ie^{-i\pi/10}\phi^{-1/2} & 0 \\ -ie^{-i\pi/10}\phi^{-1/2} & -\phi^{-1} & 0 \\ 0 & 0 & -e^{-2\pi i/5} \end{pmatrix} \tag{2.28}$$

With these two matrices any braid can be performed. This is a topic which we will get back to in the last section of this chapter, when topological quantum computation is discussed.

The basic concepts of 2-dimensional physics have been introduced in this section. Included are the possible statistics of anyons and the interaction of braiding and fusion between the particles together with their associated quantum numbers. Associativity of the fusion rules leads to the F-matrices which are maps between different bases of the n-particle Hilbert space. Together with the R-matrices, which interchange particles, any generator of the braid group can be represented by a combination of the R- and F-matrices. Up until now, we have only dealt with the theory of topological phases. It would be desirable to actually create a system that is in a topological phase; that is what the next section is concerned with.

2.2 Quantum Hall systems

Having introduced the main features of quantum statistics in 2-dimensional physics, we will use this section to present a physical system where it is expected that anyonic properties might be observed in experiments. Quantum Hall physics is a rich field, but we will be rather short on it in the following. For more details we would like to refer to the literature [5].

2.2.1 Quantum Hall effect

In 1879 Hall discovered a phenomenon observed in electrical conductors. This is nowadays known as the *Hall effect*. When an electric field is applied to a conductor, the electrons start flowing in the direction of this field, which leads to a current. However, when a perpendicular magnetic field is applied the Lorentz force comes into play. This results in a component of the current

which is orthogonal to the direction of the electric field. In short, this is what is called the Hall effect.

Nowadays the experiments on the Hall effect are done in 2-dimensional electron gases (2DEG), at low temperature, $\sim 10mK$ and subject to a strong perpendicular magnetic field, $\sim 10T$. The resistivity tensor is defined through a relation between the effective electric field $\vec{E}$ and the current $\vec{J}$

$$E^\mu = \rho_{\mu\nu} J^\nu \tag{2.29}$$

Due to arguments based on translational invariance it can be shown that for the Hall effect ρ and its inverse, the conductivity tensor σ, are given by [6]

$$\rho = \frac{B}{nec}\begin{pmatrix} 0 & 1 \\ -1 & 0 \end{pmatrix}, \qquad \sigma = \frac{nec}{B}\begin{pmatrix} 0 & -1 \\ 1 & 0 \end{pmatrix} \tag{2.30}$$

where n is the electron density and B the strength of the magnetic field, which is perpendicular to the plane. One remarkable result is that since $\sigma_{xx} = 0$ and $\rho_{xx} = 0$ the system is a perfect insulator and a perfect conductor in the direction of the electric field at the same time. The Hall resistivity is defined as $\rho_H = \rho_{xy}$ and is given by

$$\rho_H = \frac{B}{nec} \tag{2.31}$$

According to these results the Hall resistance R_H should grow linearly with the magnitude of $\vec{B}$. However, this does not agree with experimental data. In 1980 von Klitzing et al. observed what is now known as the integer quantum Hall (IQH) effect [7]. The graph of the Hall resistance shows plateaus at certain values of the magnetic field, which is shown in Fig. 2.11. Actually, this figure shows more than just the Hall plateaus found by von Klitzing et al. The plateaus denoted by an integer are part of the IQH effect. We also see plateaus at fractional values, this is known as the FQH effect, which will be discussed in later parts of this subsection. Since experiments show that (2.31) is not correct at the plateaus, it should be rewritten as

$$\rho_H = \frac{1}{\nu}\frac{h}{e^2} \tag{2.32}$$

where ν takes on integer values and is called the *filling fraction*, which we will get back to at a later stage. For now we see that plateaus form at integer

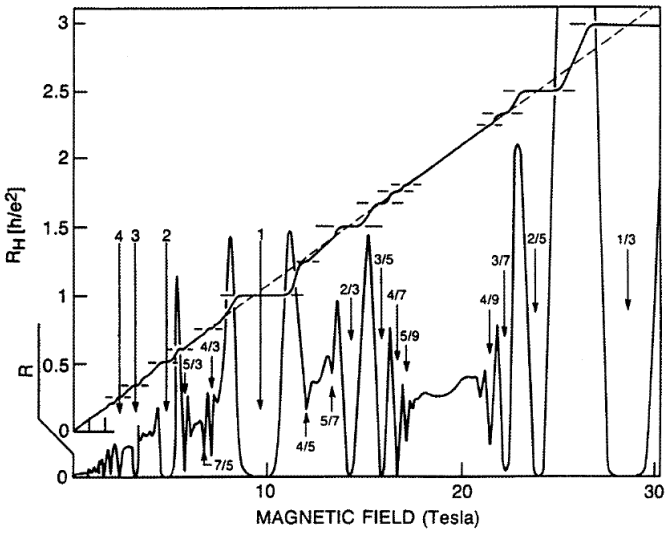

Figure 2.11: *The Hall resistance R_H is plotted against the strength of the perpendicular magnetic field. The diagonal line is what is expected from theory for an ideal 2DEG. At certain values of B, observations do not agree with this, we see stable plateaus forming. This is the integer and fractional quantum Hall effect. Also plotted is the resistance in the longitudinal direction, which drops to zero at these plateaus. Graph taken from Ref. [8].*

values of the filling fraction. This means that even though B increases the resistance does not grow.[3]

The filling fraction of the quantum Hall effect can be better understood by solving the hamiltonian for free electrons with mass m subject to a perpendicular magnetic field of strength B. This leads to Landau energy levels

$$E_n = (n + \frac{1}{2})\hbar\omega_c, \qquad n = 0, 1, ... \tag{2.33}$$

with the classical cyclotron frequency $\omega_c = \frac{eB}{mc}$. In principle, these levels are infinitely degenerate. However, since the electrons take up a finite amount of space and in experiments samples always have a finite area A, the number of available states for the electrons N_Φ in a Landau level must also be finite and given by

$$N_\Phi = \frac{ABe}{hc} = \frac{AB}{\Phi_0} \tag{2.34}$$

[3] Also, the longitudinal resistivity, ρ_{xx} drops to zero.

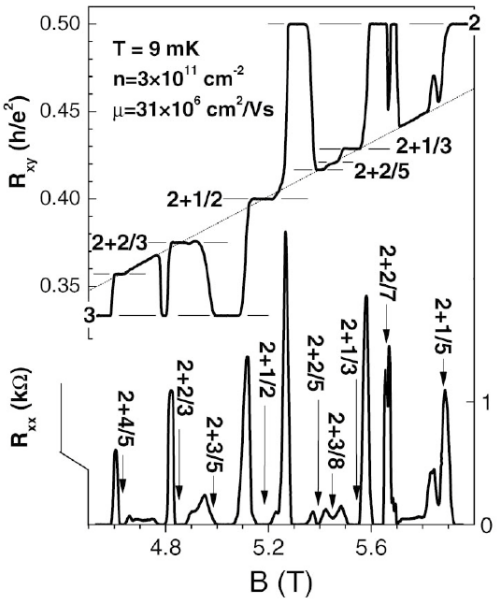

Figure 2.12: *FQH plateaus in the second Landau level appear when the Hall resistance R_{xy} is plotted as a function of the magnetic field. Note that there is a plateau for $\nu = 5/2$ which has an even denominator. Graph taken from Ref. [9].*

where $\Phi_0 = \frac{hc}{e}$, is the fundamental flux quantum. Apparently, the number of available states in a finite sample is given by the number of flux quanta piercing through its surface. Quite logically the filling fraction is defined as the number of electrons over the number of available states

$$\nu = \frac{N_e}{N_\Phi} \tag{2.35}$$

Whenever ν is an integer the Landau levels are exactly filled. Now we can understand why a quantum Hall fluid at integer filling fraction is called *incompressible*. At $\nu \in \mathbb{N}$ compressing the fluid, i.e. decreasing the area, forces some electrons to go to a higher Landau level, which costs energy. Since the spacing between different levels is $\hbar\omega_c \propto B$, for a very strong magnetic field the energy gap between the Landau levels becomes large. And the amount of energy that it costs to push an electron to a higher level is significant. For this reason the quantum Hall fluid is an incompressible state. Notice that the huge energy gap separates the multi-particle ground state from the excited states, which makes it a topological phase of matter.

So far nothing prohibits ν of being different from an integer. This happens when random impurities in the 2DEG are taken into account. Almost all electrons become localized and only a few are extended. It is precisely these extended states that can carry the current from one side of the sample to the other. When the magnetic field is tuned in such a way that it affects the localized states nothing happens; the Hall conductance stays constant, thus we are at a plateau. When it reaches the energy level of the extended states the Hall conductance suddenly increases.

This seemed like a satisfactory explanation of what is observed in the laboratory. However, trying to get devices cleaner led to the discovery of the FQH effect. In 1982 Tsui et al. observed stable plateaus at fractional filling fractions [10]. These plateaus are shown in Fig. 2.11 and they all have odd denominator filling fraction. However, experiments done in the second Landau level also show even denominator filling fractions [11, 12]. A graph with a plateau at $\nu = 5/2$ is shown in Fig. 2.12.

In trying to explain the IQH effect, one big assumption has been made and that is neglecting the Coulomb interaction between the different electrons. This assumption was legitimate since the samples used in experiments had large impurity potentials. As samples have less disorder this assumption is no longer valid and the Coulomb interaction has to be taken into account. We will not go into detail on the theory behind the FQH effect. In stead, we simply mention that FQH states are observed and that they are incompressible, like the integer states. Furthermore, the ground state is also separated from the excited states by a large gap.

Most importantly, excitations in these FQH states have fractional charge and are also expected to have fractional (and even non-Abelian) statistics. This will be discussed briefly in the next subsection where we will present some states that have been proposed to explain the physics at certain FQH plateaus.

2.2.2 FQH states

There have been many wave functions proposed to explain the physics at the Hall plateaus. We will use this subsection to mention a few of them.

Wave functions to describe the physics for the plateaus at $\nu = 1/m$, where m is an odd integer, have been proposed by Laughlin in Ref. [13]. Excitations over the ground state are quasiparticles and quasiholes and each of them is attached to one flux quantum. For N electrons and n quasiholes at complex coordinates z_i and u_j, respectively, the wave function is

$$\psi_m(z_1,...z_N;u_1,...u_n)=\prod_{i<j}(z_i-z_j)^m\prod_{k,l}(z_k-u_l)e^{-\frac{1}{4}\sum_p|z_p|^2} \tag{2.36}$$

The quasiholes have fractional charge $Q=e/m$ and when the position of two quasiparticles is interchanged it leads to a phase factor of $e^{i\pi/m}$, which implies that the quasiholes have fractional statistics $\frac{\theta}{\pi}=\frac{1}{m}$.

As can be seen from Fig. 2.11 and 2.12 the Laughlin wave functions cannot account for all observed filling fractions. All odd denominator filling fractions in the lowest Landau level can be explained by a construction now known as the Haldane-Halperin (HH) hierarchy [14, 15]. A hierarchy of states is built on top of the Laughlin state by letting the quasiparticle excitations condense into a new Laughlin-type state of matter. This hierarchy will be discussed in more detail in chapter 5.

Another series of states has been proposed by Jain in Ref. [16]. It presents a new approach of understanding the FQH effect. He argues that it can be understood as the IQH effect but for composite fermions instead of real electrons. A composite fermion is an electron attached to an even number of flux quanta, $2n$.[4] The flux quanta that are bound cannot contribute to the magnetic field, which leads to a different effective magnetic field. Starting from an IQH plateau at $\nu=p$ and assuming that the N_e electrons each bind to $2n$ flux quanta this leads to a filling fraction of the composite fermion state

$$\nu'=\frac{p}{2np\pm1}\qquad n,p\in\mathbb{N} \tag{2.37}$$

The sign depends on the relative direction of the magnetic field and the flux quanta attached to the electrons. The fundamental particle has charge $Q=e/(2np\pm1)$ and statistics $\theta/\pi=1/(2np\pm1)$. Note that for $p=1$ the Laughlin state is obtained. The composite fermion approach naturally gives a beautiful interpretation of the FQH effect in terms of the IQH effect. The down side of these states is that they do not reproduce all odd denominator filling fractions, but for the most stable values of ν they do.

The Read-Rezayi (RR) states that have been proposed in Ref. [17] are yet another series of states. The filling fractions are[5]

[4] An even number is needed to preserve fermionic statistics.

[5] The RR state for $k=3$ and $M=1$ has a sector with the same quantum numbers as the Fibonacci anyon.

$$\nu_{RR} = \frac{k}{kM+2} \qquad M = 1, 3, ..., \quad k = 1, 2, ... \tag{2.38}$$

The Moore-Read (MR) state is a special case of the RR states for $k = 2$ and $M = 1$. In Ref. [18] Moore and Read suggest a wave function to account for $\nu = 1/2$, which is a candidate for $\nu = 5/2$ in the second Landau level. The RR states have quasiparticle excitations with fractional charge and non-Abelian fractional statistics which makes them extremely interesting for TQC. We will return to the MR state in several other parts of this thesis.

Having introduced several candidate states to describe the physics of the FQH effect, we devote the last part of this section to some experiments that have been done in order to determine the charge and statistics of the excitations in FQH fluids.

2.2.3 Experiments on FQH systems

Many states have been proposed to account for the physics that is observed in FQH fluids. To verify which state is actually the correct description more experiments have to be performed.

Electric charges of quasiparticles for different filling fractions have been measured, for instance by so called shot noise experiments. The authors of Ref. [19] measured a quasiparticle charge of $e^* = e/3$ at filling fraction $\nu = 1/3$ and in Ref. [20] a charge of $e^* = e/5$ was observed for $\nu = 2/5$. These observations agree with the predicted charge of the Laughlin state and the state proposed by Jain, respectively. A similar experiment has been performed by th authors of Ref. [21]. They measured quasiparticle charges for QH fluids in the second Landau level. Most interestingly they observed a charge $e^* = e/4$ for the plateau at $\nu = 5/2$. This agrees with the predictions of Moore and Read. For details on the set up of these experiments we refer to the literature.

What is more difficult to measure, but of great interest, is the statistics of the quasiparticles. Many possible set ups have been proposed in the literature based on interference measurements for Abelian as well as non-Abelian particles, see for example Ref. [23, 24, 25]. The authors of Ref. [22] claim to have actually measured the statistics of the Laughlin quasiparticle at $\nu = 1/3$. They construct an interferometer by surrounding an island at $\nu = 2/5$ by a quantum Hall fluid at $\nu = 1/3$ (see Fig. 2.13). Tunneling between the two edges can occur upon which the quasiparticles can circle on

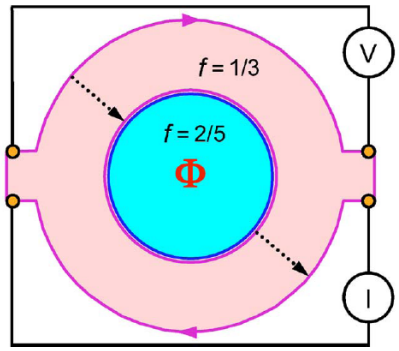

Figure 2.13: *Device used to measure the statistics of the e/3 Laughlin quasiparticles. An island at filling fraction $\nu = 2/5$ is surrounded by a quantum fluid at $\nu = 1/3$. Tunneling between the two edges can occur. When an e/3 particle tunnels to the inner edge it goes around the island and picks up a phase due to interactions with the quasiparticles on the island. If this happens interference should be measured. Figure taken from Ref. [22].*

the inner edge. This could lead to a phase factor because of interaction with the quasiparticles present on the island. The particles that tunneled have a different phase factor than the particles moving on the outer edge, which results in interference. The authors measure such an interference term, from which they draw the conclusion that the quasiparticles indeed have $\frac{\theta}{\pi} = \frac{1}{3}$ statistics,[6] which confirms the predictions of Laughlin. The same authors repeated the experiment using the same set up, but this time letting the island be at $\nu = 1/3$ as well as the surrounding fluid (see Ref. [26]). Again they find superperiods which confirm the 1/3 statistics.

Even though these experiments have been performed, it remains problematic to measure the statistics of quasiparticles. It would be especially interesting to know the statistics of the Hall fluid at $\nu = 5/2$, since this could answer the question of which of the proposed states is the right one. For instance, the MR state predicts quasiholes that have non-Abelian statistics. We will see that these non-Abelian anyons are precisely what is needed to perform topological quantum computations. The last section of the present chapter, addresses this topic.

[6] In chapter 5 we discuss a different interpretation of this result.

2.3 Topological quantum computation

This section treats topological quantum computation. Let us start with discussing quantum computation (QC) in general before we turn to the topological variant of it. The idea of doing computations by using the properties of quantum mechanics goes back to the early 1980s [1]. It was shown that QC could speed up calculations for certain problems. Even though much effort has been put into the theory of QC it remains difficult to actually build a quantum computer. The main problem is that the information that is stored decoheres quite easily, which leads to errors in the calculations. One way to deal with this problem is to develop error correcting codes; if an error occurs it can be detected and fixed. Another possibility of avoiding decoherence, is by using topological properties. Since topology is a non-local property the quantum information should not be sensitive to any local perturbations.

2.3.1 Qubits and gates

The idea behind QC is that we use a state that is in a superposition to encode a qubit

$$|\psi_i\rangle = \alpha|0\rangle + \beta|1\rangle, \qquad \text{with } |\alpha|^2 + |\beta|^2 = 1 \tag{2.39}$$

The Hilbert space spanned by this state is 2-dimensional. The way of doing calculations with such qubits is by acting on $|\psi_i\rangle$ with unitary transformations to obtain some final state $|\psi_f\rangle$ which can be read out.

The form of (2.39) suggests that non-Abelian anyons are a natural way to encode qubits. When two anyons a and b are fused their product is

$$|\psi_i\rangle = a \times b = \sum_c N_{ab}^c c \tag{2.40}$$

This is a d-dimensional Hilbert space where $d = \sum_c N_{ab}^c$. We want to act on this state by a unitary transformation to do quantum computations. Since we are dealing with a topological phase the only way that this system can undergo a transformation is by braiding anyons [1]. The unitary gates we are looking for must be accomplished by braiding anyons. Since two anyons cannot change their fusion channel by braiding, the state in (2.40) does not suffice. Extra anyons are needed to make them change their fusion channel.

How this can be done will be illustrated in the next subsection where we, yet again, use the Fibonacci model as an example.

2.3.2 TQC with Fibonacci anyons

In subsection 2.1.5 the Fibonacci model was presented. We used it to explicitly show the concepts that were discussed in the first section of this chapter. Now we will again use it as an example, but this time to illustrate TQC.

The only non-trivial particle in the Fibonacci model is the τ particle and we will use it to encode a qubit. As was mentioned, two anyons cannot change their fusion channel, so we need at least three Fibonacci anyons. Their fusion product is as follows

$$(\tau \times \tau) \times \tau = (1 + \tau) \times \tau = 1 + 2\tau \tag{2.41}$$

A system with three Fibonacci anyons has a 3-dimensional Hilbert space. Adopting notation from Bonesteel et al. in Ref. [27] where τ is represented by $\bullet$, the different states of this space can be written as follows

$$|0\rangle = |((\bullet \times \bullet)_1 \times \bullet)_\tau\rangle \tag{2.42}$$
$$|1\rangle = |((\bullet \times \bullet)_\tau \times \bullet)_\tau\rangle \tag{2.43}$$
$$|NC\rangle = |((\bullet \times \bullet)_\tau \times \bullet)_1\rangle \tag{2.44}$$

The $|0\rangle$ and $|1\rangle$ are the two orthogonal states of the qubit and $|NC\rangle$ is a noncomputational state. By braiding the three particles around each other their initial state can be changed. For the $|NC\rangle$ state we need to demand that it does not have an amplitude at the start nor at the end of the calculations. The effect of braiding can be found by determining the matrices representing the braid generators. These have been calculated and are given in (2.27) and (2.28). Note that they are block diagonal which implies that the noncomputational state does not mix with the qubit state.

The question remains if any computation can be done by using these two matrices. It turns out that the Fibonacci anyons allow for universal QC [28], which means that any unitary operation can be approximated with arbitrary precision by successively acting with $\rho(\sigma_1)$ and $\rho(\sigma_2)$. Still, it is

not trivial to find a particular unitary gate of interest. The authors of Ref. [27] present a method to find specific quantum gates to arbitrary precision.

Since TQC is not sensitive to local perturbations one might wonder if there are other ways in which errors could occur. In Ref. [1] it is discussed that errors could arise when the braiding is not done accurately. One has to keep track of positions of all the anyons in the system in order to avoid braiding of anyons that should not be involved in the calculation.

In this chapter we introduced some concepts that arise in planar physics. For instance, the statistics of particles changes dramatically when they are confined to two spatial dimensions. Instead of just fermions and bosons there is the notion of anyons. These are particles which have the property that upon interchanging two identical anyons the wavefunction describing the system acquires a phase factor that can have any value. Anyons with different statistics correspond to different irreps of the braid group. This group acts on a two dimensional system of identical particles by interchanging them.

The anyons carry two quantum numbers which will be important for later parts of this thesis. This is the quantum dimension and the topological spin. The former is closely related to the fusion rules of the anyons and the latter to rotation of an anyon over a 2π angle. These concepts are made explicit by treating an example: the Fibonacci model.

A physical system in which anyons arise are FQH fluids. This is a 2DEG subject to a strong perpendicular magnetic field and at very low temperatures. When an electric field is applied for certain values of the magnetic field the system becomes incompressible. It is exactly at these values that the QH fluid is in a topological phase and its excitations are presumably anyonic. Many states have been proposed in the literature to capture the observed physics of these phases. To test which description is correct experiments have been done to measure the charge and statistics of the excitations. So far, it seems that most of the phases have Abelian anyons, but some could also have non-Abelian excitations.

The last section deals with an implementation of anyonic systems. Non-

Abelian particles can act as a quantum register. Qubits are encoded by using the Hilbert space spanned by the fusion product of non-Abelian anyons and computations are performed by braiding these anyons. This leads to a fault-tolerant way of storing and manipulating information.

Having set the stage, in the next chapter we move on to topological symmetry breaking.

CHAPTER 3

Symmetry breaking by Bose condensation

To investigate phase transitions in a 2-dimensional topological medium we use the method of topological symmetry breaking. In many fields of physics symmetry breaking is a natural way to describe phase transitions. The idea is that the initial symmetry is broken down to a residual symmetry, which describes the new phase. For a 2D topological phase of matter anyonic quantum statistics naturally arises as we have seen in the previous chapter. The algebra that should describe the symmetry of the topological phase is different from a standard (Lie) group or algebra in that they also should incorporate the non-trivial braiding interaction that the excitations may have. The fact is that the symmetry of the system is described by a quantum group. The irreps of this quantum group label the spectrum of topological excitations. Instead one could also use the full CFT description to describe a quantum system. But writing down explicit wave functions is usually difficult. Instead we prefer the quantum group approach, i.e. the symmetries of the system, because the method is very general and allows us to extract what we want to know in a systematic way.

This chapter will give an extensive overview of the concept of topological symmetry breaking set out in Ref. [4, 29, 30, 31]. We will use this scheme to induce transitions between different topological phases. This enables us to describe the degrees of freedom present in the bulk of the different phases as well as on the boundary between them. The steps that need to be taken are

roughly the following: First identify the spectrum of the initial phase by labeling the excitations by irreps of the underlying quantum group. Next, find a bosonic excitation in this spectrum and assume that it forms a condensate, upon fusion with this condensate certain fields will become identified and others will split, all of this is captured by the branching rules. Now we have reached a new intermediate phase described by a $\mathcal{T}$-algebra that has good fusion rules, but where non-consistent braiding might arise. Excitations that do not braid trivially with the condensed excitations will pull strings in the condensate and due to energy considerations will be expelled from the bulk and must live on the boundary of the phase. Lastly, we recognize that the fields that are unconfined make up a new, final phase, described by an algebra $\mathcal{U}$. These excitations are the true particle-like excitations of the broken phase. By following these steps we have a phase transition between an initial phase described by a quantum group $\mathcal{A}$ and a final phase described by $\mathcal{U}$. The domain wall between the two phases can be fully captured by the intermediate $\mathcal{T}$-algebra.

The second section of the present chapter is structured after these three steps. To illustrate how this process works in practice we discuss an explicit phase transition while presenting the general framework. As an example we choose Kitaev's honeycomb model described in Ref. [32]. Before we reach this point we start with a brief introduction to quantum groups and how they describe the underlying symmetry of a 2D quantum system.

3.1 Quantum groups

The previous chapter showed that the braid group acts non-trivially on a 2-dimensional system. The appearance of the braid group can be associated with an underlying symmetry described by a quantum group $\mathcal{A}$. This is a special case of a Hopf algebra which is a generalization of groups. For a precise discussion and exact definitions of quantum groups we refer to the literature on quantum groups [33, 34].

It suffices to mention that each excitation in the spectrum of a topological phase carries an irrep of a quantum group that describes the symmetry of the system. So the spectrum is obtained when we know the irreps of the quantum group. The extra structure that quantum groups have are such that the physical properties of the excitations like fusion and braiding can correctly be taken into account.

For instance, there is a structure called the coproduct which makes it able to act on a multi-particle state, i.e. it allows for a consistent definition of how

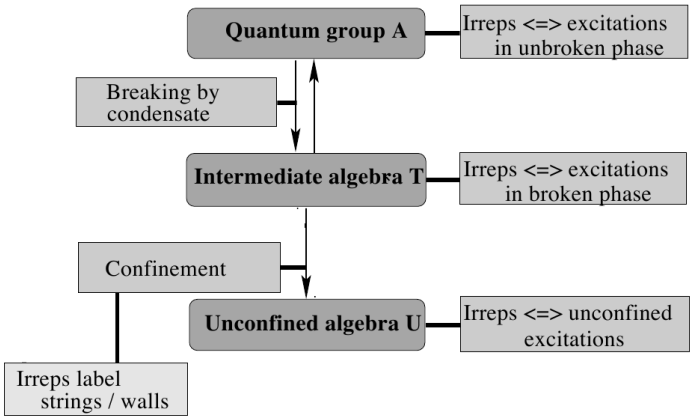

Figure 3.1: *Topological symmetry breaking happens in two steps. Our initial phase has an underlying symmetry denoted by a quantum group $\mathcal{A}$. The spectrum of this phase is labeled by the irreps of $\mathcal{A}$. After a condensate of bosonic quasiparticles forms the symmetry breaks down to a smaller algebra $\mathcal{T} \subset \mathcal{A}$. The excitations in this phase might not have well-defined braiding statistics with the condensate. Those which do not braid trivially pull strings in the condensate and will become confined to the boundary of the system. We are left with a final algebra $\mathcal{U}$ describing excitations that are closed under fusion and have well-defined braiding statistics.*

the quantum group acts on a tensor product state of two representations. Given that action one can deduce how the product representation reduces into irreducible components and that way gives rise to the tensor product of fusion rules of representations. The R-matrix which was introduced in the previous chapter is the operator that implements the braid operation on a two-particle state. In the quantum group language this operator corresponds with a canonical element in the tensor product of the algebra with itself. This particular element has the important property that it commutes with the action of the quantum group $\mathcal{A}$ and therefore by considering tensor products we can always decompose any product of n irreps into irreducible representations of the product $\mathcal{A} \otimes \mathcal{B}_n$.

In the following we will work with quantum systems of which we know the spectrum and fusion and braiding interactions, i.e. we identify the physical system by the collection of representations and their labels. This is usually the case with physical applications of abstract algebraic structures. This means that we will not write down the explicit quantum groups, but just assume that they describe the underlying symmetry. We will see that for the examples we are considering this is sufficient.

3.2 Phase transitions

The main idea of topological symmetry is sketched in Fig. 3.1. The breaking happens in two steps. Our initial phase has an underlying symmetry denoted by a quantum group $\mathcal{A}$. The spectrum of this phase is labeled by the irreps of $\mathcal{A}$. The first step is when a condensate of bosonic particles forms. This condensate breaks the symmetry down to a smaller algebra $\mathcal{T} \subset \mathcal{A}$. Again the spectrum of this intermediate phase is labeled by irreps of $\mathcal{T}$. This is an intermediate phase since the excitations in this phase might not have well-defined braiding statistics with the condensate. Those which do not braid trivially pull strings in the condensate and will become confined to the boundary of the system. This leads us to the last step where we reach a final phase with excitations labeled by irreps of an algebra $\mathcal{U}$ which are closed under fusion and have well-defined braiding statistics.

3.2.1 Getting started

First thing that needs to be done is identifying the excitation spectrum of the topological phase we are studying. Since this is a rather general statement we will immediately move to the example we chose to discuss, namely Kitaev's honeycomb model.

This is a model where spin-1/2 particles live on the sites of a honeycomb lattice. They have nearest neighbor interactions and this model can be solved exactly. Depending on the different coupling strengths there are four different phases. Three of these phases have an energy gap and carry Abelian anyons that have the same order as the $\mathbb{Z}_2$ toric code, which is the same as the quantum double $D(\mathbb{Z}_2) = \mathbb{Z}_2 \otimes \mathbb{Z}_2$ [4]. The fourth phase is gapless,

Ising

$c = 1/2$	1	σ	ψ
h_i	0	$\frac{1}{16}$	$\frac{1}{2}$
d_i	1	$\sqrt{2}$	1

$\sigma \times \sigma = 1 + \psi$	$\psi \times \psi = 1$
$\sigma \times \psi = \sigma$	

$\mathbb{Z}_2$ toric code

$c = 0$	1	e	m	em
h_i	0	0	0	1/2
d_i	1	1	1	1

$e \times e = 1$	$m \times m = 1$
$em \times em = 1$	$e \times m = em$
$m \times em = e$	$em \times e = m$

Table 3.1: *Sectors of the Ising model (left) and $\mathbb{Z}_2$ toric code (right) together with their spins, quantum dimensions and the fusion rules of the non-trivial sectors. The fusion rules are commutative.*

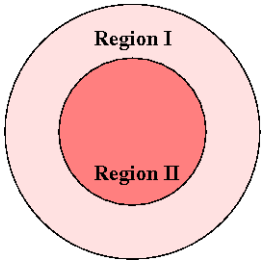

Figure 3.2: *Phase diagram with two different topological phases.*

but becomes gapped in the presence of a magnetic field. The excitations of this phase are non-Abelian and turn out to be the same as the sectors of the Ising model. The field content of the Ising model and $\mathbb{Z}_2$ toric code are given in Tab. 3.1.

The aim is to obtain a configuration with two different phases, where one has Ising sectors and the other is the $\mathbb{Z}_2$ toric code, this is shown in Fig. 3.2. We could just bring two phases close together, but what happens at the boundary of the two? This question can be answered by following the scheme set out below.

Let us start with a disc carrying the Ising sectors. The different sectors of the Ising model together with their quantum numbers are given in Tab. 3.1. The idea is that we place a smaller auxiliary layer on top of this Ising disc and induce a phase transition in the overlapped region so that we end up with the phase we are aiming for.[1]

The conformal field theory (CFT) describing the Ising model has central charge $c = 1/2$ and the Abelian phase we are aiming for has zero central charge. It seems logical to use an auxiliary layer that cancels the central charge of the Ising part. Let us try to do it with a smaller disc carrying $\overline{Ising}$ sectors. This model has central charge $c = -1/2$ and the sectors have spins that also have opposite signs from the Ising model sectors. The fusion rules and quantum dimensions are the same for both theories.

So we place a smaller disc carrying an $\overline{Ising}$ model on top of our original Ising disc as is shown in Fig. 3.2. This just means we take a tensor product of the two theories in the region where they overlap. This region will be denoted by region II from now on. It has an underlying symmetry described by $\mathcal{A} = Ising \otimes \overline{Ising}$. The quantum dimensions of two sectors in a tensor

[1] It is not always necessary to use an auxiliary layer. If there is a bosonic excitation present in the single-layered system we could just condense it in a part of the phase in order to obtain a two-phased diagram. This has been done, for example in Ref. [4].

product multiply and the spins add up.

At this point we have an initial spectrum labeled by irreps of $\mathcal{A}$ in region II. To proceed the symmetry breaking we first have to identify a bosonic sector in region II.

3.2.2 Boson

The next step in the symmetry breaking scheme would be to form a condensate of bosonic excitations. But what is a boson in two spatial dimensions? In more than two dimensions bosons are particles that have integer spin. This is the same as the condition that exchanging two bosons leaves the system invariant. In two dimensions these two are not necessarily equal anymore.

Consider the relation between self-monodromy of a particle with trivial spin and fusion of two such particles. This is shown in Fig. 3.3 and the phase that relates these two processes is $e^{2\pi i(h_c-2h_b)} = e^{2\pi i h_c}$. From this we see that requiring invariance under braiding, there should be at least one fusion channel that has integer spin, leading to the following definition of a boson:

> Let $b \in \mathcal{A}$ with fusion rule $b \times b = \sum_c N_{bb}^c c$, if
>
> 1. $h_b \in \mathbb{Z}$
> 2. $\exists c$ with $h_c \in \mathbb{Z}$
>
> then b is a boson.

Going back to Kitaev's honeycomb model we can identify the bosons in this system. From Tab. 3.1 we see that there are two non-trivial bosons: (ψ, ψ) and (σ, σ), these are the diagonal fields. It should be clear that they both have spin equal to zero which meets the first requirement of being a boson. For the second requirement we note that their fusion rules are

$$(\psi,\psi) \times (\psi,\psi) = (1,1) \tag{3.1}$$
$$(\sigma,\sigma) \times (\sigma,\sigma) = (1,1) + (1,\psi) + (\psi,1) + (\psi,\psi) \tag{3.2}$$

Both have the vacuum in their fusion product which has zero spin. At this point we have identified what the non-trivial excitations are with Bose-statistics.

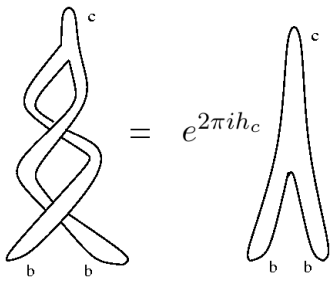

Figure 3.3: *Self-monodromy of a boson b. In order to have invariance of the system under exchange of two bosons we must demand that there is at least one fusion channel c that has integer spin.*

3.2.3 Branching rules

So far we are still in the upper bar of Fig. 3.1; it is the initial phase we are dealing with. Now is the time that we make our first step of the symmetry breaking scheme. This breaking occurs when the bosonic excitations form a condensate. We must investigate what happens to our initial spectrum when this condensate forms. The idea is that the condensate is our new vacuum so it should not interact with the other excitations in the spectrum. This means that the symmetry underlying the initial spectrum is broken and we need to determine what our new spectrum is. The present subsection is concerned with the interaction between the excitations and the condensate through fusion.

Going back to the quantum group language we note that the initial spectrum was labeled by irreps of $\mathcal{A}$. When a condensate forms the symmetry is broken down to a smaller algebra $\mathcal{T} \subset \mathcal{A}$. This algebra has irreps that might differ from the irreps of $\mathcal{A}$. What could happen is the following:

- Whenever an irrep of $\mathcal{A}$ is also an irrep of $\mathcal{T}$ the excitations labeled by it are still present in the broken phase.
- Irreps that were different under the initial symmetry could correspond to the same irrep of $\mathcal{T}$, so these excitations become identified with each other in the broken phase.
- If an irrep of $\mathcal{A}$ is not an irrep of $\mathcal{T}$ it can be written as a direct sum of representations that are irreducible under $\mathcal{T}$. This means that these excitations split up into two or more parts in the broken phase.

These three possibilities can be written in a compact form, which is called the *branching rules*

$$a \to \sum_t n_t^a t \tag{3.3}$$

where a is an irrep of $\mathcal{A}$ and t an irrep of $\mathcal{T}$. What appears after the arrow is called the *restriction* of a. The coefficient $n_t^a \in \mathbb{N}$ gives the number of times t appears. In practice we find these branching rules by fusing the excitations in the spectrum of $\mathcal{A}$ with the condensate.

Again due to physical requirements the fusion rules of this new spectrum must also be associative, there must be a unique vacuum sector, and every sector has a conjugate sector.[2] Besides this, we have to put two more constraints on the branching rules of the different sectors:

- The sector b that condenses must contain the vacuum in its branching rule: $b \to 1 + \sum_t n_t^b t$.
- Fusion rules and branching should commute. In other words fusing sectors labeled by $\mathcal{A}$ and then branching the result to $\mathcal{T}$ should be equal to branching the sectors of $\mathcal{A}$ and then fusing the sectors of $\mathcal{T}$.

A helpful tool in determining the branching rules comes from these two conditions. It can be shown that quantum dimensions are preserved under branching

$$d_a = \sum_t n_t^a d_t \tag{3.4}$$

where d_a is the quantum dimension of $a \in \mathcal{A}$ and d_t is the quantum dimension of $t \in \mathcal{T}$ which are the fields a branches to.

Returning to our model we will show how this works. Even though there are two non-trivial bosons (ψ, ψ) and (σ, σ), we will assume only the (ψ, ψ) field condenses. If we look at the fusion rules of this condensate with the other excitations that are present in the initial phase we find

[2] As an aside we mention that we do not demand consistent braiding at this point. We will see later on in this section that this enables us to describe more than just the pointlike excitations appearing after the phase transition occurred.

$$\begin{array}{lcll} (1,1) & \times & (\psi,\psi) & = & (\psi,\psi) \\ (\psi,1) & \times & (\psi,\psi) & = & (1,\psi) \\ (\sigma,1) & \times & (\psi,\psi) & = & (\sigma,\psi) \\ (1,\sigma) & \times & (\psi,\psi) & = & (\psi,\sigma) \\ (\sigma,\sigma) & \times & (\psi,\psi) & = & (\sigma,\sigma) \end{array} \tag{3.5}$$

The condensed field is a *simple current* of order 2. A simple current J is a sector that has unit quantum dimension from which it follows that fusing J with any other sector results in only one fusion channel [4]. The order p of a simple current is defined through $J^{\times p} = 1$. This means that the orbits under fusion with (ψ,ψ) have a maximum length of 2. From which it follows that the first eight fields in (3.5) get pairwise identified, but the (σ,σ) field is invariant under fusion with the condensate. Writing this in terms of branching rules, this looks like

$$\begin{array}{lcl} (1,1),(\psi,\psi) & \to & (1,1) \\ (1,\psi),(\psi,1) & \to & (\psi,1) \\ (\sigma,1),(\sigma,\psi) & \to & (\sigma,1) \\ (1,\sigma),(\psi,\sigma) & \to & (1,\sigma) \\ (\sigma,\sigma) & \to & (\sigma,\sigma)_1 + (\sigma,\sigma)_2 \end{array} \tag{3.6}$$

Let us see why we have these particular branching rules. The first four lines of (3.6) can be explained by looking at the quantum dimensions of the fields at the left hand side, they all have $d_i < 2$. Since the quantum dimension of a sector needs to be at least 1 and quantum dimensions are preserved under branching it follows that the restriction of these sectors can only have one part. Of the two fields that become pairwise identified we choose one of those to label the restriction of them.[3] The last line of (3.6) is a bit more complicated since (σ,σ) has quantum dimension $d = 2$, so in priciple it could split. Take a look at the fusion rule of this field with itself

$$\begin{array}{rcl} (\sigma,\sigma)\times(\sigma,\sigma) & = & (1,1)+(1,\psi)+(\psi,1)+(\psi,\psi) \\ & \to & 2(1,1)+2(\psi,1) \end{array} \tag{3.7}$$

Since the restriction contains the vacuum twice (σ,σ) needs to split, otherwise there is no unique way in which they annihilate. That the restriction

[3] We could have chosen totally new labels, but if we want to keep track of the correspondence of sectors in $\mathcal{A}$ and $\mathcal{T}$ this is the easiest way to accomplish it.

$Ising \otimes \mathbb{Z}_2$	$(1,1)$	$(\psi,1)$	$(\sigma,1)$	$(1,-1)$	$(\psi,-1)$	$(\sigma,-1)$
$\mathcal{T}$	$(1,1)$	$(\psi,1)$	$(\sigma,1)$	$(1,\sigma)$	$(\sigma,\sigma)_1$	$(\sigma,\sigma)_2$
	$(\psi,1)$	$(1,1)$	$(\sigma,1)$	$(1,\sigma)$	$(\sigma,\sigma)_2$	$(\sigma,\sigma)_1$
	$(\sigma,1)$		$(1,1)+(\psi,1)$	$(\sigma,\sigma)_1+(\sigma,\sigma)_2$	$(1,\sigma)$	$(1,\sigma)$
	$(1,\sigma)$			$(1,1)+(\psi,1)$	$(\sigma,1)$	$(\sigma,1)$
	$(\sigma,\sigma)_1$				$(1,1)$	$(\psi,1)$
	$(\sigma,\sigma)_2$					$(1,1)$

Table 3.2: *Fusion rules of the intermediate $\mathcal{T}$-algebra corresponding to the broken phase of $Ising \otimes \overline{Ising}$. These sectors have $Ising \otimes \mathbb{Z}_2$ fusion rules, which is made explicit by the top most line.*

has precisely two fields directly follows from the quantum dimension being equal to 2.

The six fields at the right hand side of (3.6) make up the spectrum of the broken phase that is described by $\mathcal{T}$. The fusion rules of these fields are given in Tab. 3.2 and turn out to be the same as $Ising \otimes \mathbb{Z}_2$.

At this point we have taken the first step of the symmetry breaking scheme, shown in Fig. 3.1, by letting bosonic sectors form a condensate which breaks the symmetry to a new algebra $\mathcal{T}$. This broken phase is closed under fusion but we have not demanded consistent braiding and spins so far.

3.2.4 Confinement

The condensate should not interact with the other excitations in the spectrum. The previous subsection took care of fusion interaction. To take the last step of the symmetry breaking shown in Fig. 3.1 we need to look at the braiding interaction of the different sectors in the spectrum with the condensate.

Let us look at the monodromy of a sector a with the condensate b when are in fusion channel c, this is shown in Fig. 3.4. If there should not be any braiding interaction we have to demand

$$e^{2\pi i(h_c - h_a)} = 1 \quad \Leftrightarrow \quad h_c - h_a \in \mathbb{Z} \tag{3.8}$$

To give a precise definition of which sectors have non-trivial braiding interaction with the condensate we first need to define the notion of *lifts* of a

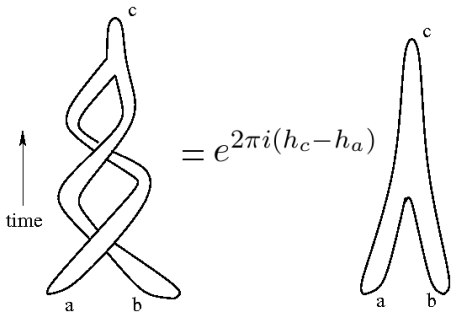

Figure 3.4: *There is no braiding interaction between the condensate b and sector a as long as* $h_c - h_a \in \mathbb{Z}$.

sector

The lifts of a sector $\tilde{t} \in \mathcal{T}$ are the sectors $a \in \mathcal{A}$ that have $\tilde{t}$ in their restriction:

$$a \to n_{\tilde{t}}^a \tilde{t} + \sum_t n_t^a t$$

for nonzero $n_{\tilde{t}}^a$

Now that we defined the lifts of a sector in the broken phase we are able to define which sectors in this broken phase must become confined.

If the lifts of a sector $t \in \mathcal{T}$ do not have equal spin factors then this sector is confined

What does it mean when a field becomes confined? To answer this question we will sketch an intuitive picture of confinement. The condensate can be viewed as some background field. Just like the usual vacuum it can be considered everywhere. If a particle is placed in the condensate it should leave the condensate invariant, otherwise it does not belong to the spectrum of this system. Let us assume that this particle braids non-trivially with the particles forming the condensate. Instead of writing a phase factor we shall denote braiding by some intrinsic orientation of the particles. The condensate has such an intrinsic orientation. If a particle is placed in the condensate this orientation will continuously change going around the particle, but it should go back to its initial value at a 2π angle. If it does not then the order parameter of the condensate has a line singularity terminating in the particle and it is not continuous anymore. This results in a branch cut

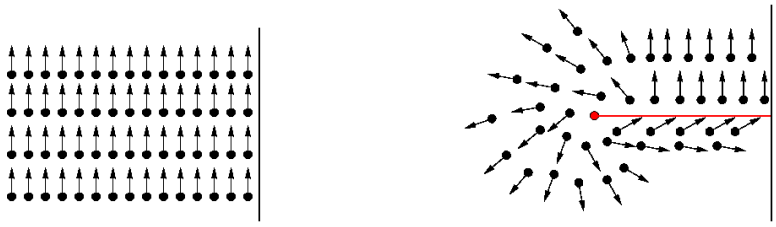

Figure 3.5: *Left figure shows the order parameter of the condensate as arrows pointing up. Bringing a particle into the condensate changes this order parameter. When this particle braids non-trivially with the condensate there will be a branch cut in the condensate. Physically this means that the particle pulls a string attached to the boundary of the system.*

which costs a certain amount of energy. Fig. 3.5 visualizes a particle that pulls a string in the condensate. To minimize energy the particle will be driven out of the bulk and will reside on the boundary of the system.

So we see that the fields that become confined are driven out of the bulk of region II and must sit on the boundary between this region and region I shown in Fig. 3.2.[4]

Going back to to the honeycomb model we identify which of the six fields in the intermediate $\mathcal{T}$-algebra will be confined. The fields of $\mathcal{T}$ are listed in Tab. 3.3, together with their lifts in the unbroken phase and the difference in spin between these lifts. The criterium for confinement tells us that the fields $(\sigma, 1)$ and $(1, \sigma)$ are confined.

$\mathcal{T}$	Lifts	h_{dif}
$(1,1)$	$(1,1),(\psi,\psi)$	2
$(\psi,1)$	$(\psi,1),(1,\psi)$	1
$(\sigma,1)$	$(\sigma,1),(\sigma,\psi)$	1/2
$(1,\sigma)$	$(1,\sigma),(\psi,\sigma)$	1/2
$(\sigma,\sigma)_1$	(σ,σ)	0
$(\sigma,\sigma)_2$	(σ,σ)	0

Table 3.3: *Determining which fields in $\mathcal{T}$ become confined, we look at the difference in spin of their lifts. These are shown in the last column. Whenever this difference is an integer the corresponding field will be unconfined in the broken phase.*

[4] There is a possibility for confined sectors to form a hadronic composite, which can live in the bulk. This happens when at least two confined sectors are joined together by their strings and have a combined charge that is unconfined. The $\mathcal{T}$-algebra has to be invoked to determine which hadrons are possible.

3.2.5 Effective theory

After the expulsion of the confined sectors we are left with an unconfined broken theory in region II. This is the effective theory which has a certain spectrum with underlying symmetry described by an algebra $\mathcal{U}$. All the excitations in this spectrum are closed under fusion and have well-defined braiding interactions. We have arrived at the last station of the symmetry breaking process displayed in Fig. 3.1.

Using this method we know which degrees of freedom are present in both regions of Fig. 3.2. Besides this we also know what happens on the interface between the two regions. This is a very important statement. In the beginning of this section it was discussed that trying to explain a system with two different topological phases just by bringing the separate phases close together fails to reproduce what processes happen on the boundary where the phases meet. The approach of symmetry breaking produced such a two-phased diagram and tells us what happens on the interface.

This power comes from the intermediate $\mathcal{T}$-algebra. It can be used to describe the excitations of region II by noting that these are just the unconfined fields. The excitations of region I correspond to a $\mathcal{T}$ field modulo fusion with the condensate. Then there are the wall excitations. Again these are also fully described by the $\mathcal{T}$-algebra. They are the fields that are confined in the broken theory and cannot be identified with an excitation from region I. These sectors are strictly confined to the wall, since they cannot move into the bulk of region I nor the bulk of region II.

Another comment can be made concerning the $\mathcal{T}$-algebra. It describes a spectrum that is closed under fusion, but does not have well-defined braiding statistics. Now we see that this is not a problem after all. Since the $\mathcal{T}$-algebra describes the excitations that live on the boundary, it is quite logical that it does not exhibit well-defined braiding. The boundary of a two dimensional system is one dimensional. So it is clear that no consistent braiding is possible on this interface.

Returning to Kitaev's honeycomb model for the last time, we note that there are four unconfined fields present in the bulk of region II. Looking at their spins, quantum dimensions and fusion rules we see that these are the same as the $\mathbb{Z}_2$ toric code. This means that going back to Fig. 3.2 we have produced this phase diagram where region I has Ising sectors and region II has the same order as the $\mathbb{Z}_2$ toric code.[5] The link between the excitations in

[5] Note that we assumed that only (ψ, ψ) formed a condensate. But there was another non-trivial boson. Had we also demanded (σ, σ) to condense then we had found a diagram with region I described by Ising and region II would have been just the vacuum.

$Ising$ (region I)	$\mathcal{T}-algebra$ (I/II wall)	$\mathbb{Z}_2$ *toric code* (region II)
1	$(1,1)$	1
ψ	$(\psi,1)$	em
σ	$(\sigma,1)$	
	$(1,\sigma)$	
	$(\sigma,\sigma)_1$	e
	$(\sigma,\sigma)_2$	m

Table 3.4: *First column shows the fields that can move into the bulk of region I. The third column displays the fields moving into the bulk of region II. Both have their corresponding $\mathcal{T}$ field in the second column.*

these two regions and their corresponding field of the $\mathcal{T}$-algebra is listed in Tab. 3.4. This table also shows us that even though there were two confined fields in the broken theory only one of them is a true boundary excitation. The $(\sigma,1)$ field was confined, thus driven out of the bulk of region II, but it can move into the bulk of region I. On the other hand, $(1,\sigma)$ cannot move into region I, so it has to stay on the wall between the two regions.

Note that there is one sector that can move freely through the whole phase diagram, namely $(\psi,1)$. In region I it is identified with ψ and in region II with em.

It is also interesting to consider some processes involving $(1,\sigma)$ that could occur:

- When two wall excitations $(1,\sigma)$ fuse they may form a $(\psi,1)$ excitation, which can move into the bulk of either region I as a ψ field or region II as a em field, i.e. $(1,\sigma)\times(1,\sigma)=(1,1)+(\psi,1)$.
- A $(1,\sigma)$ field can split into a σ field and either a e or m field, i.e. $(1,\sigma)\in(\sigma,1)\times(\sigma,\sigma)_i$.

These final statements take us to the end of this chapter. What we did is in-

troduce the concept of topological symmetry breaking. This happens when a bosonic excitation in the spectrum forms a condensate. Consequently, the degrees of freedom need to be rearranged such that fields that differ by fusion with the condensed particle are identified with each other. This new spectrum is described by an intermediate symmetry. The last step is concerned with the braiding interaction of the excitations with the condensate. When an excitation braids non-trivially with the bosonic particles it pulls a string in the condensate and will become confined to the boundary of the system. This leaves us with a final phase that has a spectrum of excitations with well-defined fusion and braiding interactions. The symmetry breaking scheme can be used to describe a system that has different topological phases separated by a boundary. In this way we can pin down all the degrees of freedom that are present in those phases as well as on the interface between them.

This rather technical concept has been applied to a simple, but instructive model, namely Kitaev's honeycomb model. We constructed a phase diagram where region I carries non-Abelian Ising sectors and region II is Abelian with the same order as the $\mathbb{Z}_2$ toric code. It turns out that there is one excitation that is strictly confined to the boundary between both regions and one excitation can move freely in both phases. Also we discussed two specific fusion and splitting processes.

The rest of this thesis will be on applying topological symmetry breaking to FQH states, we first study a specific case of interest and later will talk about understanding complete hierarchies of states from our condensate point of view.

CHAPTER 4

Interface between non-Abelian FQH states

The first part of this thesis was concerned with presenting the basic concepts behind planar physics and with topological symmetry breaking. Now is the time that we put all of this into practice. We do this by considering several explicit topological phases of matter. This chapter will deal with a system that has two different topological phases. Both phases are non-Abelian FQH states. The first is the MR state which is a spin polarized state. This state was proposed to describe the observed quantum Hall plateau at filling fraction $\nu = 5/2$. The excitations have a non-Abelian part that has the same sectors as the Ising model and a chiral boson corresponding to electric charge. The second phase is the non-Abelian spin-singlet (NASS) state at $\nu = 4/7$ [35]. The excitations in this phase also carry a non-Abelian part which are $SU(3)_2/U(1)^2$ parafermions and an Abelian part consisting of two chiral bosons carrying charge and spin. A system with these two phases was also considered in Ref. [36]. The authors obtained a partition sum for the edge between the two phases by using the 'giant hole approach'. They write down a counting formula for NASS on a sphere and start adding spin up quasiholes on a part of this sphere. In this way they create a MR state in this region. Also there has been proposed a method in Ref. [37] where 1-dimensional anyonic spin chains lead to a 2-dimensional system with two different phases that have this initial spin chain as the gapless excitations of the boundary. At the end of this chapter we will compare our results to the results of these references.

Ising

$c = 1/2$	1	σ	ψ
h_i	0	$\frac{1}{16}$	$\frac{1}{2}$
d_i	1	$\sqrt{2}$	1
$\sigma \times \sigma = 1 + \psi \quad \psi \times \psi = 1$			
$\sigma \times \psi = \sigma$			

Table 4.1: *Sectors of the Ising model together with their spins, quantum dimensions and fusion rules.*

We will use topological symmetry breaking as described in chapter 3 to obtain such a two-phased system. This is done by adding an auxiliary layer to an MR phase. It will be shown that there is a bosonic excitation and we condense it upon which the symmetry of the system is broken. After determining the branching rules of the different sectors and the confinement we will see that the final phase is described by the NASS state. The results presented here have been published in a paper in collaboration with Bais and Slingerland [38].

4.1 Constructing the two-phased system

Let us start this section by once again stressing the difficulty in obtaining a system which has more than one topological phase. We cannot just bring two phases close together to create a boundary between them. This would not tell us what happens exactly at this boundary. Instead we use symmetry breaking to go from one phase to the other. If we are able to set our parameters in such a way that only a part of the system breaks its symmetry and thus undergoes a phase transition we create a system with two regions carrying different topological phases.

To accomplish a system where region I is in the MR state and region II in the NASS state we want to add an auxiliary layer to MR and start the symmetry breaking scheme. We will only be considering the non-Abelian parts of the theory since the chiral bosons can be put back in at any time.

In order to choose what auxiliary layer should be used, we look at the central charge of the different CFT's describing the phases. The Ising CFT has central charge $c = 1/2$ and the parafermions of NASS have $c = 6/5$. The difference between the two is $7/10$. It would sound like a natural choice to choose an auxiliary layer that has a CFT with central charge $c = 7/10$.

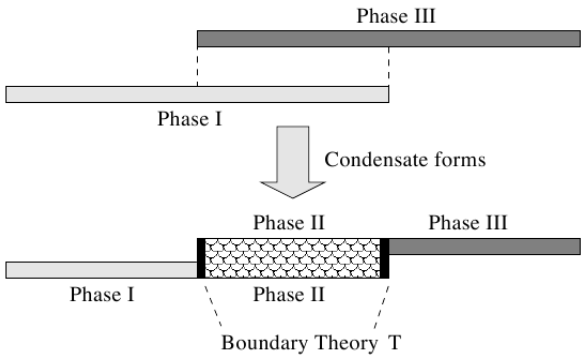

Figure 4.1: *Start with phase I which carries Ising sectors. Partially let it overlap with phase III described by $\mathcal{M}(4,5)$. In the region where they overlap a condensate may form which leads to a new phase II carrying NASS excitations.*

There is a minimal model denoted by $\mathcal{M}(4,5)$, which is also called the tricritical Ising model,[1] that has exactly this central charge [39].

This tells us that we should start with a phase described by the Ising model and a phase carrying sectors of $\mathcal{M}(4,5)$. The sectors, their quantum numbers, and the fusion rules are listed in Tab. 4.1 and 4.2. Let the two theories partially overlap which means that we take the tensor product of the two models in this sector, see Fig. 4.1. This region is described by

$$\mathcal{A} = Ising \otimes \mathcal{M}(4,5) \tag{4.1}$$

$\mathcal{A}$ has 18 different sectors, that are given in Tab. 4.3. Also listed are their quantum dimensions and spins. It shows that there is only one non-trivial boson in this $\mathcal{A}$-algebra: (ψ, ϵ'').

$$\begin{aligned} &h_{(\psi,\epsilon'')} \in \mathbb{Z} \\ &(\psi,\epsilon'') \times (\psi,\epsilon'') = (1,1) \end{aligned} \tag{4.2}$$

We see that this is a sector with spin factor equal to 1 and trivial self-monodromy, thus it is a boson.

[1] The Ising model is also a minimal model, namely $\mathcal{M}(3,4)$.

$\mathcal{M}(4,5)$

$c = 7/10$	1	ϵ	ϵ'	ϵ''	$\tilde{\sigma}$	$\tilde{\sigma}'$
h_i	0	$\frac{1}{10}$	$\frac{3}{5}$	$\frac{3}{2}$	$\frac{3}{80}$	$\frac{7}{16}$
d_i	1	$\frac{1+\sqrt{5}}{2}$	$\frac{1+\sqrt{5}}{2}$	1	$\frac{1+\sqrt{5}}{\sqrt{2}}$	$\sqrt{2}$

	ϵ	$1+\epsilon'$				
	ϵ'	$\epsilon+\epsilon''$	$1+\epsilon'$			
	ϵ''	ϵ'	ϵ	1		
	$\tilde{\sigma}$	$\tilde{\sigma}+\tilde{\sigma}'$	$\tilde{\sigma}+\tilde{\sigma}'$	$\tilde{\sigma}$	$1+\epsilon+\epsilon'+\epsilon''$	
	$\tilde{\sigma}'$	$\tilde{\sigma}$	$\tilde{\sigma}$	$\tilde{\sigma}'$	$\epsilon+\epsilon'$	$1+\epsilon''$

Table 4.2: *Spins, quantum dimensions and fusion rules of the tricritical Ising model* $\mathcal{M}(4,5)$

4.1.1 Broken theory

Now we assume that this bosonic sector forms a condensate and in this way the $\mathcal{A}$-theory is broken. This means that the condensate branches to the vacuum of the theory described by a smaller symmetry $\mathcal{T}$. Since (ψ, ϵ'') has unit quantum dimension it has no other sectors in its branching rules besides the vacuum. We find the other sectors of the $\mathcal{T}$-theory by looking at the fusion rules of the condensate with the sectors in the spectrum of $\mathcal{A}$. This is relatively easy since the condensed sector is a simple current of order 2, which leads to orbits under fusion with (ψ, ϵ'') containing a maximum of two sectors. The orbits are as follows

$\mathcal{A} = Ising \otimes \mathcal{M}(4,5)$

sector	h_i	d_i	*sector*	h_i	d_i	*sector*	h_i	d_i
$(1,1)$	0	1	$(\sigma,1)$	$\frac{1}{16}$	$\sqrt{2}$	$(\psi,1)$	$\frac{1}{2}$	1
$(1,\epsilon)$	$\frac{1}{10}$	$\frac{1+\sqrt{5}}{2}$	(σ,ϵ)	$\frac{13}{80}$	$\frac{1+\sqrt{5}}{\sqrt{2}}$	(ψ,ϵ)	$\frac{3}{5}$	$\frac{1+\sqrt{5}}{2}$
$(1,\epsilon')$	$\frac{3}{5}$	$\frac{1+\sqrt{5}}{2}$	(σ,ϵ')	$\frac{53}{80}$	$\frac{1+\sqrt{5}}{\sqrt{2}}$	(ψ,ϵ')	$\frac{11}{10}$	$\frac{1+\sqrt{5}}{2}$
$(1,\epsilon'')$	$\frac{3}{2}$	1	(σ,ϵ'')	$\frac{25}{16}$	$\sqrt{2}$	(ψ,ϵ'')	2	1
$(1,\tilde{\sigma})$	$\frac{3}{80}$	$\frac{1+\sqrt{5}}{\sqrt{2}}$	$(\sigma,\tilde{\sigma})$	$\frac{1}{10}$	$1+\sqrt{5}$	$(\psi,\tilde{\sigma})$	$\frac{43}{80}$	$\frac{1+\sqrt{5}}{\sqrt{2}}$
$(1,\tilde{\sigma}')$	$\frac{7}{16}$	$\sqrt{2}$	$(\sigma,\tilde{\sigma}')$	$\frac{1}{2}$	2	$(\psi,\tilde{\sigma}')$	$\frac{15}{16}$	$\sqrt{2}$

Table 4.3: *Sectors of $\mathcal{A}$-theory: $Ising \otimes \mathcal{M}(4,5)$. Clearly, (ψ, ϵ'') is the only non-trivial boson candidate.*

$$\begin{array}{lcll}
(1,1) & \times & (\psi,\epsilon'') & = (\psi,\epsilon'') \\
(1,\epsilon) & \times & (\psi,\epsilon'') & = (\psi,\epsilon') \\
(1,\epsilon') & \times & (\psi,\epsilon'') & = (\psi,\epsilon) \\
(1,\epsilon'') & \times & (\psi,\epsilon'') & = (\psi,1) \\
(1,\tilde{\sigma}) & \times & (\psi,\epsilon'') & = (\psi,\tilde{\sigma}) \\
(1,\tilde{\sigma}') & \times & (\psi,\epsilon'') & = (\psi,\tilde{\sigma}') \\
(\sigma,1) & \times & (\psi,\epsilon'') & = (\sigma,\epsilon'') \\
(\sigma,\epsilon) & \times & (\psi,\epsilon'') & = (\sigma,\epsilon') \\
(\sigma,\tilde{\sigma}) & \times & (\psi,\epsilon'') & = (\sigma,\tilde{\sigma}) \\
(\sigma,\tilde{\sigma}') & \times & (\psi,\epsilon'') & = (\sigma,\tilde{\sigma}')
\end{array} \tag{4.3}$$

These orbits have a maximal order of two, so the above fusion rules give all the information needed to find the identifications which will lead to the $\mathcal{T}$-algebra. The first eight rows each give two fields that get identified with each other. This means that they have the same restriction when we look at their branching rules. Furthermore they can only branch to a single sector, since their quantum dimensions are all less than 2. The last two rows need to be considered more closely. These two sectors get mapped to itself by the bosonic sector. If we look at the fusion rules of those sectors we see that

$$\begin{array}{lcl}
(\sigma,\tilde{\sigma}) \times (\sigma,\tilde{\sigma}) & = & (1,1) + (\psi,1) + (1,\epsilon) + (\psi,\epsilon) + (1,\epsilon') + \\
 & & (\psi,\epsilon') + (1,\epsilon'') + (\psi,\epsilon'') \\
 & = & 2(1,1) + 2(1,\epsilon'') + 2(1,\epsilon) + 2(1,\epsilon') \\
(\sigma,\tilde{\sigma}') \times (\sigma,\tilde{\sigma}') & = & (1,1) + (\psi,1) + (1,\epsilon'') + (\psi,\epsilon'') \\
 & = & 2(1,1) + 2(1,\epsilon'')
\end{array} \tag{4.4}$$

Since both sectors contain the vacuum twice this means they must split. It turns out that it is sufficient to split both into two parts

$$\begin{array}{lcl}
(\sigma,\tilde{\sigma}) & \to & (\sigma,\tilde{\sigma})_1 + (\sigma,\tilde{\sigma})_2 \\
(\sigma,\tilde{\sigma}') & \to & (\sigma,\tilde{\sigma}')_1 + (\sigma,\tilde{\sigma}')_2
\end{array} \tag{4.5}$$

This follows from the fact that three parts would result in at least nine fusion channels when they are fused with themselves. When we consider (4.4) they both have less fusion channels than this, so they must split into precisely two parts. Furthermore, the restrictions of $(\sigma,\tilde{\sigma})$ and $(\sigma,\tilde{\sigma}')$ cannot be be identified with the vacuum, since the vacuum in (4.4) appears only twice. This means that the restrictions have to be non-trivial sectors. Also, this implies that the two fields in the restriction cannot be equal to each other. The branching rules of all the sectors of the initial $\mathcal{A}$-algebra are

$$\begin{array}{lcl}
(1,1),(\psi,\epsilon'') & \to & (1,1) \\
(1,\epsilon),(\psi,\epsilon') & \to & (1,\epsilon) \\
(1,\epsilon'),(\psi,\epsilon) & \to & (1,\epsilon') \\
(1,\epsilon''),(\psi,1) & \to & (1,\epsilon'') \\
(1,\tilde{\sigma}),(\psi,\tilde{\sigma}) & \to & (1,\tilde{\sigma}) \\
(1,\tilde{\sigma}'),(\psi,\tilde{\sigma}') & \to & (1,\tilde{\sigma}') \\
(\sigma,1),(\sigma,\epsilon'') & \to & (\sigma,1) \\
(\sigma,\epsilon),(\sigma,\epsilon') & \to & (\sigma,\epsilon) \\
(\sigma,\tilde{\sigma}) & \to & (\sigma,\tilde{\sigma})_1+(\sigma,\tilde{\sigma})_2 \\
(\sigma,\tilde{\sigma}') & \to & (\sigma,\tilde{\sigma}')_1+(\sigma,\tilde{\sigma}')_2
\end{array} \tag{4.6}$$

Note that we choose to label the sectors of the intermediate $\mathcal{T}$-algebra in the same way as we labeled their lifts. We could have chosen a totally new set of labels, but now we are able to keep track of the correspondence between $\mathcal{A}$ and $\mathcal{T}$. We get a surjective map from $\mathcal{A}$ onto $\mathcal{T}$.

The intermediate $\mathcal{T}$-algebra has a spectrum with 12 different sectors. Let us try to assign quantum dimensions to those sectors. Since quantum dimension is preserved under branching the first eight sectors of (4.6) will inherit the quantum dimension of their lifts. For the same reason and the fact that $(\sigma,\tilde{\sigma}')$ has quantum dimension equal to 2, it follows that $(\sigma,\tilde{\sigma}')_1$ and $(\sigma,\tilde{\sigma}')_2$ both must have unit quantum dimension. Looking at the product $(\sigma,\tilde{\sigma})\times(\sigma,1)=2(1,\tilde{\sigma})$ we can conclude that the two sectors in the restriction of $(\sigma,\tilde{\sigma})$ must have equal quantum dimensions, which means they will have quantum dimension equal to $\frac{1+\sqrt{5}}{2}$.

sector	h_i	d_i	*sector*	h_i	d_i
$(1,1)$	0	1	$(\sigma,\tilde{\sigma}')_1$	$\frac{1}{2}$	1
$(1,\epsilon)$	$\frac{1}{10}$	$\frac{1+\sqrt{5}}{2}$	$(\sigma,\tilde{\sigma})_1$	$\frac{1}{10}$	$\frac{1+\sqrt{5}}{2}$
$(1,\epsilon')$	$\frac{3}{5}$	$\frac{1+\sqrt{5}}{2}$	$(\sigma,\tilde{\sigma})_2$	$\frac{1}{10}$	$\frac{1+\sqrt{5}}{2}$
$(1,\epsilon'')$	$\frac{3}{2}$	1	$(\sigma,\tilde{\sigma}')_2$	$\frac{1}{2}$	1
$(1,\tilde{\sigma})$	$confined$	$\frac{1+\sqrt{5}}{\sqrt{2}}$	(σ,ϵ)	$confined$	$\frac{1+\sqrt{5}}{\sqrt{2}}$
$(1,\tilde{\sigma}')$	$confined$	$\sqrt{2}$	$(\sigma,1)$	$confined$	$\sqrt{2}$

Table 4.4: *$\mathcal{T}$-algebra of the broken $Ising\otimes\mathcal{M}(4,5)$ theory. Sectors that cannot be assigned a spin factor become confined.*

The sectors of the $\mathcal{T}$-algebra are listed in Tab. 4.4 together with their quantum dimensions. Not all of those sectors can be assigned spins though. For instance, take the lifts of $(1,\tilde{\sigma})$, which are $(1,\tilde{\sigma})$ and $(\psi,\tilde{\sigma})$. They have spin $\frac{3}{80}$ and $\frac{43}{80}$, respectively. This means they do not have equal spin factors

and so they must become confined. It is impossible to find a known quantum group that is the same as this T-algebra, since not all sectors have spin. This is not really a problem since our T-theory has a 1-dimensional interpretation as explained before. So there is no such thing as braiding and spins have no meaning in this context.

Even though the spin factors cannot be assigned, we can determine the fusion rules of the $\mathcal{T}$ sectors. On every line of Tab. 4.4 there are two sectors with the same quantum dimension. This suggests that we must be looking for an algebra of the form "$2 \otimes 6$". Where the 2 stands for an algebra with two sectors both having the same quantum dimension and 6 has six sectors. It turns out that the algebra that does the job is $\mathbb{Z}_2 \otimes \mathcal{M}(4,5)$. This can be seen as follows. The sectors in the first column of Tab. 4.4 are evidently the elements $(1, \mathcal{M}(4,5))$. Now we need a sector from the second column that corresponds to the non-trivial element of $\mathbb{Z}_2$, namely -1. This means that upon fusion of this field with the fields in the first column of Tab. 4.4 we get the fields in the second column. It turns out that we have two options: both $(\sigma, \tilde{\sigma}')_1$ and $(\sigma, \tilde{\sigma}')_2$ have this property. Choose $(\sigma, \tilde{\sigma}')_1 \to (-1, 1) \in \mathbb{Z}_2 \otimes \mathcal{M}(4,5)$

$$\begin{array}{lcllcl}
(1,1) & \times & (\sigma,\tilde{\sigma}')_1 & = & (\sigma,\tilde{\sigma}')_1 & \to & (-1,1) \\
(1,\epsilon) & \times & (\sigma,\tilde{\sigma}')_1 & = & (\sigma,\tilde{\sigma})_1 & \to & (-1,\epsilon) \\
(1,\epsilon') & \times & (\sigma,\tilde{\sigma}')_1 & = & (\sigma,\tilde{\sigma})_2 & \to & (-1,\epsilon') \\
(1,\epsilon'') & \times & (\sigma,\tilde{\sigma}')_1 & = & (\sigma,\tilde{\sigma}')_2 & \to & (-1,\epsilon'') \\
(1,\tilde{\sigma}) & \times & (\sigma,\tilde{\sigma}')_1 & = & (\sigma,\epsilon) & \to & (-1,\tilde{\sigma}) \\
(1,\tilde{\sigma}') & \times & (\sigma,\tilde{\sigma}')_1 & = & (\sigma,1) & \to & (-1,\tilde{\sigma}')
\end{array} \tag{4.7}$$

We see that this produces all the fields of the $\mathcal{T}$-algebra. The explicit fusion rules of $\mathcal{T}$ are given in appendix A. So the $\mathcal{T}$-algebra is equal to $\mathbb{Z}_2 \otimes \mathcal{M}(4,5)$ on the level of the fusion rules. Once more we would like to stress that the spin factors are not the same as those of $\mathbb{Z}_2 \otimes \mathcal{M}(4,5)$.

4.1.2 Effective theory: NASS

The last step will lead to the effective theory of region II as was shown in Fig. 4.1. The underlying symmetry is denoted by a $\mathcal{U}$-algebra. To obtain this the sectors that do not have well-defined spins must be left out. These sectors are driven out of the bulk of region II and are confined to the boundary.

Tab. 4.4 shows that four sectors of the broken theory must become confined and that we are left with eight sectors in the broken unconfined phase.

$\mathcal{U}$	$(1,1)$	$(\sigma,\tilde{\sigma})_1$	$(\sigma,\tilde{\sigma})_2$	$(1,\epsilon)$	$(1,\epsilon')$	$(\sigma,\tilde{\sigma}')_1$	$(\sigma,\tilde{\sigma}')_2$	$(1,\epsilon'')$
NASS	1	$\sigma_\uparrow$	$\sigma_\downarrow$	σ_3	ρ	ψ_1	ψ_2	ψ_{12}
h_i	0	$\frac{1}{10}$	$\frac{1}{10}$	$\frac{1}{10}$	$\frac{3}{5}$	$\frac{1}{2}$	$\frac{1}{2}$	$\frac{1}{2}$
d_i	1	$\frac{1+\sqrt{5}}{2}$	$\frac{1+\sqrt{5}}{2}$	$\frac{1+\sqrt{5}}{2}$	$\frac{1+\sqrt{5}}{2}$	1	1	1
	$\sigma_\uparrow$	$1+\rho$						
	$\sigma_\downarrow$	$\psi_{12}+\sigma_3$	$1+\rho$					
	σ_3	$\psi_1+\sigma_\downarrow$	$\psi_2+\sigma_\uparrow$	$1+\rho$				
	ρ	$\psi_2+\sigma_\uparrow$	$\psi_1+\sigma_\downarrow$	$\psi_{12}+\sigma_3$	$1+\rho$			
	ψ_1	σ_3	ρ	$\sigma_\uparrow$	$\sigma_\downarrow$	1		
	ψ_2	ρ	σ_3	$\sigma_\downarrow$	$\sigma_\uparrow$	ψ_{12}	1	
	ψ_{12}	$\sigma_\downarrow$	$\sigma_\uparrow$	ρ	σ_3	ψ_2	ψ_1	1

Table 4.5: *$\mathcal{U}$-algebra turns out to be the same as the non-Abelian part of the NASS state. Listed are the different sectors, their quantum numbers, and fusion rules.*

Looking at the fusion rules, spins, and quantum dimensions of these sectors we can conclude that they are the same as those of the sectors that make up the non-Abelian part of the NASS state, see Tab. 4.5.

At this point we have a full description of the system we were aiming for, namely one that has an interface between the NASS and MR state. But the minimal model $\mathcal{M}(4,5)$ can also be included in this picture. Now we obtain a diagram with three different phases as shown in Fig. 4.2. The field content of these phases are given in Tab. 4.6. It shows us which sectors are present in the bulk of the three phases. This is also written in terms of the tensor product that came from the initial $\mathcal{A}$-algebra $Ising \otimes \mathcal{M}(4,5)$. The last two lines of the table are of special interest. It tells us which excitations are strictly confined to the boundary between the phases. We get a non-trivial description of what happens at a phase transition. The $\mathcal{T}$-algebra serves as

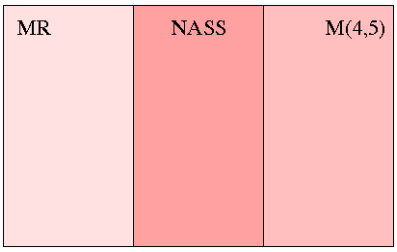

Figure 4.2: *System carrying three topological phases. The boundaries between the phases are described in a non-trivial way by the $\mathcal{T}$-algebra. The different fields in the bulk and on the boundaries are given in Tab. 4.6.*

$\mathcal{T}-theory$	1	$\sigma_\uparrow$	$\sigma_\downarrow$	σ_3	ρ	ψ_1	ψ_2	ψ_{12}	σ	$\tilde{\sigma}$	$\tilde{\sigma}'$	σ^*
$Lifts\ in$	$(1,1)$	$(\sigma,\tilde{\sigma})$		$(1,\epsilon)$	$(1,\epsilon')$	$(\sigma,\tilde{\sigma}')$		$(1,\epsilon'')$	$(\sigma,1)$	$(1,\tilde{\sigma})$	$(1,\tilde{\sigma}')$	(σ,ϵ)
$Ising\otimes\mathcal{M}(4,5)$	(ψ,ϵ'')			(ψ,ϵ')	(ψ,ϵ)			$(\psi,1)$	(σ,ϵ'')	$(\psi,\tilde{\sigma})$	$(\psi,\tilde{\sigma}')$	(σ,ϵ')
MR	1							ψ	σ			
$NASS$	1	$\sigma_\uparrow$	$\sigma_\downarrow$	σ_3	ρ	ψ_1	ψ_2	ψ_{12}				
$\mathcal{M}(4,5)$	1			ϵ	ϵ'			ϵ''		$\tilde{\sigma}$	$\tilde{\sigma}'$	
$MR/NASS$										$\tilde{\sigma}$	$\tilde{\sigma}'$	σ^*
$NASS/\mathcal{M}(4,5)$									σ			σ^*

Table 4.6: *Spectra of the different phases. The $\mathcal{T}$-theory is the dictionary between the different phases and is shown in the top most line. The line below gives the sectors that correspond to these $\mathcal{T}$ sectors written as a tensor product of the initial $\mathcal{A}$-algebra. The third, fourth and fifth line give the sectors that are allowed in the bulk of respectively MR, NASS and $\mathcal{M}(4,5)$. The last two lines show which excitations are strictly confined to either the wall between MR and NASS or the wall between NASS and $\mathcal{M}(4,5)$.*

a dictionary in this case. The fusion rules of $\mathcal{T}$ together with Tab. 4.6 give us all the fusion and splitting processes that could possibly occur anywhere in the diagram shown in Fig. 4.2.

4.2 Kinematics

In the previous section it was shown how to construct a configuration with one region described by the MR state and the other by the NASS state. This approach supplied us with a full description of the topological excitations in the bulk of the two regions as well as the excitations that are strictly confined to the boundary between the two regions. We know what fusion and splitting processes are possible and what the braiding statistics are.

4.2.1 Splitting of a quasihole

We could consider many fusion and splitting processes, but let us use this subsection to concentrate on one particular splitting process, namely the decay of a spin-up quasihole ($\sigma_\uparrow$) on the NASS side. There are a couple of scenarios which we can identify by looking for fusion products that have $\sigma_\uparrow$ as an element. We have divided the fusion products that reach this requirement up into five categories:

1. $1\times\sigma_\uparrow$, $\psi_{12}\times\sigma_\downarrow$, $\rho\times\psi_2$, $\rho\times\sigma_\uparrow$, $\sigma_3\times\sigma_\downarrow$, $\sigma_3\times\psi_1$
   These products happen solely on the NASS side. They are not that

interesting since we did not need our whole breaking scheme to accomplish these results.

2. $\epsilon'' \times \sigma_\downarrow$, $\epsilon' \times \psi_2$, $\epsilon' \times \sigma_\uparrow$, $\epsilon \times \sigma_\downarrow$, $\epsilon \times \psi_1$
   All those fusion products come from taking the product of an $\mathcal{M}(4,5)$ excitation with a NASS excitation. Even so, these are not that relevant either. This is because the $\mathcal{M}(4,5)$ excitations are not truly confined to the wall. They are identified with fields on the NASS side so there is no reason for them to stay on the wall, e.g. $\epsilon'' \times \sigma_\downarrow$ corresponds to $\psi_{12} \times \sigma_\downarrow$. Effectively this is the same as category 1.

3. $\psi \times \sigma_\downarrow$
   Here we are dealing with an excitation on the Ising side times an excitation on the NASS side. However, the Ising sector (ψ) corresponds to a NASS sector (ψ_{12}) so it might as well stay on the NASS side of the diagram.

4. $\tilde{\sigma}' \times \sigma^*$, $\tilde{\sigma} \times \sigma^*$
   Finally we have reached a case that is of special interest. These two products both happen on the wall. But this time the fields are true wall excitations, i.e. they cannot move to the NASS side nor to the Ising side. This means that whenever we drag the spin-up quasihole through the boundary it might split up into two boundary excitations.

5. $\tilde{\sigma} \times \sigma$
   The last category is one where upon dragging $\sigma_\uparrow$ through the boundary it might split up into an Ising quasihole (σ) and a true boundary-excitation ($\tilde{\sigma}$).

Evidently the last two categories are of special interest and are shown in Fig. 4.3. They contain the Ising-, $\mathcal{M}(4,5)$- and NASS-theory in a non-trivial way.

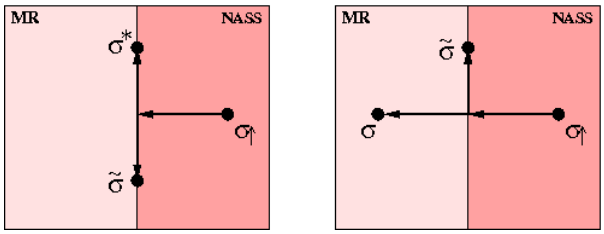

Figure 4.3: *Both figures show the dragging of a spin-up quasihole through the boundary. The left figure corresponds to category 4 where the quasihole splits up into two excitations that are strictly confined to the boundary. The right figure shows a process where it splits up into a boundary excitation and a quasihole on the Ising side.*

Such an analysis can be done for all the sectors of the different phases and the boundary. Even though a splitting process was considered, it should be clear that the different fusion processes can be obtained in a similar fashion.

4.2.2 Qubit relaxation

As has been discussed before in section 2.3 we can use topological phases to do quantum computations or to act as a quantum register. The excitations of such phases are used to encode qubits and the logical gates are implemented by braiding these quasiparticles. Since we describe two non-Abelian phases in this chapter we can try to encode a qubit in these phases.

Tab. 4.6 together with the fusion rules and spins of these sectors tells us if we can encode a qubit in this system. On the Ising side a qubit can be encoded using two quasiholes: $\sigma \times \sigma = 1 + \psi$, they can either fuse to the vacuum or to the Majorana fermion. When there are two qubits like this the Hilbert space is 2-dimensional, since topological charge is conserved. Creating four quasiholes from the vacuum implies that they must ultimately fuse to the vacuum again. So if the first qubit fuses to 1, the second must also fuse to 1, but they could also both fuse to ψ and then to 1. This is shown in Fig. 4.4. Even though we can make certain logical gates by braiding these quasiparticles, the Ising model is not suitable for universal quantum computation, when we only allow braiding of the particles [1].

The fusion rules of the NASS excitations show us that they have a Fibonacci structure when we note that [40]

$$1 \leftrightarrow \{1, \psi_1, \psi_2, \psi_{12}\} \qquad \tau \leftrightarrow \{\sigma_\uparrow, \sigma_\downarrow, \sigma_3, \rho\} \tag{4.8}$$

As has been shown in subsection 2.3.2 the Fibonacci model does allow for universal quantum computation. There are several possibilities to encode a qubit on the NASS side, for instance

$$\sigma_\uparrow \times \sigma_\downarrow = \psi_{12} + \sigma_3 \tag{4.9}$$
$$\sigma_3 \times \sigma_3 = 1 + \rho \tag{4.10}$$

The authors of Ref. [25] discuss that such a qubit can always change its fusion channel by exchanging a topologically neutral particle with the edge between the vacuum. They propose a device from which it could be possible

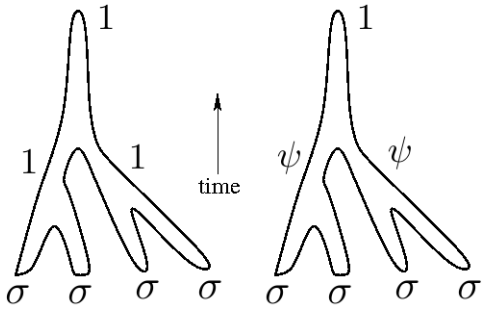

Figure 4.4: *Two qubits constitute a 2-dimensional space.*

to recognize non-Abelian statistics of the RR and NASS state. They consider electrical transport through a large quantum dot that is in the spin-singlet state. The energy of the dot is changed by slowly varying the area of the dot. When the energy in the presence of N_e electrons in the bulk of the dot coincides with the energy of $N_e + 1$ electrons a small conductance can be measured which results in so-called Coulomb blockade peaks. For an Abelian quantum Hall fluid, these peaks are evenly separated. For the NASS state there appears a periodicity in the spacing between the Coulomb blockade peaks, which is a result of the different fusion channels of the bulk quasiholes. They can change their fusion channel by exchanging ρ with the edge of the dot in order to minimize energy.

We use this idea of changing the fusion channel by exchanging a neutral particle with the edge of the system. For the Ising qubit this means that if it is in the ψ channel it can relax to the vacuum by exchanging a Majorana fermion with the boundary. For (4.9) and (4.10) the neutral particle is ρ. That these are the particles that changes the fusion channel can be seen from looking at the fusion rules. The cases of the Ising qubit and (4.10) are rather trivial since $\psi \times 1 = \psi$ and $\rho \times 1 = \rho$. For (4.9) it can be understood by noting that $\rho \times \psi_{12} = \sigma_3$. So the qubits can change their fusion channel by exchanging a neutral particle with the boundary of the system.

$$\sigma_\uparrow \overset{\rho}{\times} \sigma_\downarrow = \psi_{12} + \sigma_3 \tag{4.11}$$

But we not only have a boundary between the vacuum and a non-trivial topological phase, we also have a boundary between two different phases. To see what can happen we need to consult the fusion rules. As for the previous discussion on dragging a spin-up quasihole through the boundary,

the $\mathcal{T}$-algebra is of great importance.

Whenever a qubit on the NASS side relaxes its state by exchanging ρ with the boundary between the MR region, multiple splitting processes may occur. In principle it can split into two boundary excitations or one boundary excitation and an Ising quasihole. Both scenarios are sketched in Fig. 4.5. The two excitations drawn in the left figure can be: $\tilde{\sigma} \times \tilde{\sigma}, \tilde{\sigma} \times \tilde{\sigma}'$ and $\sigma^* \times \sigma^*$. The right figure has only $\sigma \times \sigma^*$ as a possibility. The same analysis can be done for an Ising qubit. When a Majorana fermion is exchanged with the boundary it can split up into two boundary excitations $\tilde{\sigma} \times \tilde{\sigma}$, $\sigma^* \times \sigma^*$ and $\tilde{\sigma}' \times \tilde{\sigma}'$. Also ψ can move from the boundary into the NASS region propagating as a ψ_{12} excitation.

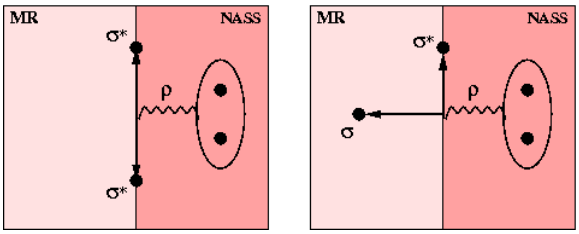

Figure 4.5: *If a qubit is encoded in the NASS region it may relax its state by exchanging a neutral ρ particle with the boundary separating this region from the MR side. This ρ particle may split up into two boundary excitations (left) where there are three possibilities of which only one is given. The other two are $\tilde{\sigma} \times \tilde{\sigma}$ or $\tilde{\sigma} \times \tilde{\sigma}'$. Also ρ can split in a boundary excitation and an Ising quasihole (right).*

4.2.3 Some thoughts

To end this chapter we would like to give a quick overview of the results of the authors in Ref. [36, 37] and some critical statements about our results.

Grosfeld and Schoutens also find the minimal model with $c = 7/10$ at the interface between MR and NASS, but they do not have the extra $\mathbb{Z}_2$ part that we find. This might be explained by the fact that they seem to throw out the gapped modes that live on the edge, although this is not mentioned explicitly in their paper. Using just the TQFT, it seems to be difficult to determine which modes will be gapped and which are gapless on the edge.

This extra $\mathbb{Z}_2$ structure that we find on the interface gives more possibilities for interface processes to occur. For example, the left figure in Fig. 4.3 is not found in Ref. [36]. This is an explicit difference between the two approaches.

Also, there is a difference in the predictions about qubit relaxation in the NASS phase. Again, this comes from the difference between the CFT and TQFT approach. It turns out that if one looks at the CFT of the NASS state the ρ field has to split into two parts $\rho \to \rho_c + \rho_s$. This comes from the fact that ρ has two independent leading Virasoro primaries which would lead to inconsistencies in the fusion rules of the primary fields if ρ would not split [40]. In Ref. [36] it is stated that ρ_c is the neutral particle that changes the fusion channel of $\sigma_3 \times \sigma_3$ and ρ_s does the same for $\sigma_\uparrow \times \sigma_\downarrow$. This leads to different boundary processes whenever such qubits relax their state. The statement of Grosfeld and Schoutens is that a $\sigma_3 \times \sigma_3$ qubit can relax its state through the interface between NASS and MR, but a spin-up/spin-down qubit can only manage to relax its state if simultaneously a $\sigma \times \sigma$ qubit in the MR region exchanges a Majorana fermion with this interface. We do not see a difference between the two qubit states in the NASS region. On the other hand we predict other boundary processes that the authors of Ref. [36] do not see.

Another subtlety we would like to mention concerns the $U(1)$ factors that were left out during the whole derivation. One would expect that there are chiral bosonic modes on the interface. The sectors of the MR state have one chiral boson and the NASS sectors have two. So it seems logical that the interface sectors would also have a chiral boson. This chiral boson could not just be any $U(1)$ factor, it should somehow depend on the MR and NASS $U(1)$ factors. We expect that keeping track of all these factors during the symmetry breaking scheme we would be able to find what the $U(1)$ factor of the interface should be. As an aside we mention that the approach in Ref. [36] does not seem to keep track of chiral bosons either; they also only focus on the parafermionic sectors. The method that the authors of Ref. [37] use does assign a $U(1)$ factor to the interface theory. But they have not considered the NASS/MR interface yet. Instead they describe a phase transition between a $SU(2)_2$ and $SU(2)_3$ liquid. The first is almost the same as the Ising model and the second has a Fibonacci structure in it. Their boundary CFT is $\mathcal{M}(4,5) \otimes U(1)$.

In this chapter we showed how to construct a configuration with two different non-Abelian FQH states. The states are the spin-polarized MR state at $\nu = 5/2$ and a spin-singlet state at $\nu = 4/7$. The method we use provides us

with a description of the bulk excitations as well as the boundary excitations. Most of those boundary excitations can move into the bulk of either one of the regions. Even so, there are three excitations that are strictly confined to the boundary and there is one excitation, which turns out to be the Majorana fermion of the MR state, that can move through the boundary into the NASS region as the ψ_{12} parafermion. We also showed how to use the fusion rules of the $\mathcal{T}$-algebra to explore what fusion and splitting processes are possible. Explicitly, we discussed dragging a spin-up quasihole from the NASS side through the boundary. We ended this chapter by commenting on the possibility of encoding a qubit consisting of two quasiholes. This can happen either in the NASS region or the MR region. Such a qubit can relax its state by exchanging a neutral particle with the boundary of the system. We see what processes may occur when such a neutral excitation is inserted on the boundary.

CHAPTER 5

A quantum group approach to FQH hierarchy picture

The previous chapter dealt with a first explicit example of a phase transition between two FQH states, induced by Bose condensation of quasiparticles. This was a transition between the MR state and NASS state. The present chapter will also be concerned with phase transitions between FQH states, but now the hierarchy picture is the case of interest. This is a picture where a new FQH state is obtained by building it on top of another FQH state. Repeating this process builds a hierarchy of states.

The aim of this chapter is to reproduce the hierarchy picture by Bose condensation. In this way we induce a phase transition between two states of some hierarchy, which can be repeated k times. Leading to $k-1$ phase transitions between k different states. Before we get to this point we start with sketching some different hierarchies in section 5.1 that have been proposed in the literature. Also Wen's K-matrix formalism is introduced which allows for a nice compact notation. In section 5.2 we consider two specific examples, namely an Abelian hierarchy at $\nu_I = 1/3$ and $\nu_{II} = 2/5$ and a non-Abelian hierarchy at $\nu_I = 5/2$ and $\nu_{II} = 12/5$. Section 5.3 will contain a construction of a general hierarchy. Again, we will discuss both the Abelian and non-Abelian case. The work described here will be published in collaboration with Bais, Bonderson and Slingerland [41].

5.1 Hierarchy picture to the FQH states

In 1983 Laughlin [13] proposed wavefunctions to describe the Hall plateaus at $\nu = 1/m$ for m an odd integer. The fundamental quasiparticles have fractional charge of $1/m$ and Abelian fractional statistics. Haldane and Halperin generalized Laughlin's scheme to a hierarchy of states with filling fraction [14, 15]

$$\nu = \cfrac{1}{m + \cfrac{\alpha_1}{p_1 + \cfrac{\alpha_2}{\ldots + \cfrac{\alpha_n}{p_n}}}} \tag{5.1}$$

where $m = 1, 3, ...,$ $\alpha_i = \pm 1$, and $p_i = 2, 4, ...$ This is now known as the Haldane-Halperin (HH) hierarchy. Clearly, the filling fraction of the Laughlin states is reproduced when $n = 0$, so the parent state of the HH-hierarchy is a Laughlin state. This hierarchy reproduces all odd denominator filling fractions of the lowest Landau level.

In Ref. [42] a different hierarchy is developed by Bonderson and Slingerland. It aims at describing the observed plateaus in the second Landau level. Explicitly they show how to build a hierarchy of states on the MR state. The hierarchization only occurs in the $U(1)$ part of the theory, implying that all daughter states will have the MR structure. They show that this Bonderson-Slingerland (BS) hierarchy provides a candidate state for all observed filling fractions in the second Landau level, including $\nu = 5/2$.

Some other non-Abelian hierarchies have been proposed such as in Ref. [43] where wavefunctions are constructed by taking correlators of vertexoperators that insert electrons and non-Abelian quasiparticles. In Ref. [44] both non-Abelian quasiholes and quasiparticles are inserted in these correlators.

$m = 3$

	$\alpha_1 = 1$	$\alpha_1 = -1$
$p_1 = 2$	$\frac{2}{7}$	$\frac{2}{5}$
$p_1 = 4$	$\frac{4}{13}$	$\frac{4}{11}$

$m = 3, \quad p_1 = p_2 = 2$

	$\alpha_1 = 1$	$\alpha_1 = -1$
$\alpha_2 = 1$	$\frac{5}{17}$	$\frac{5}{13}$
$\alpha_2 = -1$	$\frac{3}{11}$	$\frac{3}{7}$

Table 5.1: *Filling fractions of some hierarchy states for a Laughlin parent state at $\nu = \frac{1}{3}$. The left table shows the filling fractions at the first level of hierarchy. Building a second level on top of the states shown in the first row results in four new states which have filling fractions that are presented in the right table. These specific values of ν have all been observed in experiments.*

In the following we will focus on the HH and BS hierarchy. Whenever we want to describe an arbitrary level of these hierarchies it turns out to be useful to use the K-matrix formulation of Wen.

K-matrix formalism Chern-Simons theory can be used to describe FQH states. When writing down the lagrangian describing the long-distance physics of a FQH state a coupling matrix K can be extracted [45]. Many quantities like the filling fraction, quasiparticle charge, and statistics can be expressed in terms of this matrix. Also vertex operators are expressible in terms of K and consequently, wavefunctions that are constructed by taking correlators of these vertexoperators.

We will not be using the most general form of the K-matrix. Instead we choose K_{00} odd, K_{jj} even for $j > 0$, $K_{j,j+1} = K_{j+1,j} = -\mathrm{sgn}(K_{j+1,j+1})$, and all other entries are zero. The filling fraction can be expressed in terms of the K-matrix as

$$\nu = [K^{-1}]_{00} = \cfrac{1}{K_{00} - \cfrac{1}{K_{11} - \cfrac{1}{\cdots - \cfrac{1}{K_{nn}}}}} \tag{5.2}$$

This reproduces the filling fraction of the HH hierarchy. It can also be shown that for certain levels of this hierarchy we obtain the Jain series.

In section 5.3 the K-matrix formalism will be used extensively. But first we turn to two phase transitions between specific FQH states.

5.2 Phase transitions between different levels of hierarchy

In this section two different examples of a phase transition by condensation of bosonic quasiparticles are presented. First a transition between a state at $\nu = 1/3$ and a state at $\nu = 2/5$ is discussed. These states fit into the HH hierarchy, but are also part of the Jain series [16]. The second example is a transition between $\nu = 5/2$ and $\nu = 12/5$, which is the first level of the BS hierarchy. Both two-phased systems are accomplished by placing an auxiliary layer on top of the initial phase.

5.2.1 HH hierarchy at $\nu_I = \frac{1}{3}$ and $\nu_{II} = \frac{2}{5}$

The first transition that is considered is between two states of the HH hierarchy. Region I is at the zeroth level and has filling fraction $\nu_I = 1/3$. Region II is the first level of hierarchy and has $\nu_{II} = 2/5$. This is the configuration that we would like to reproduce to try to predict the different quantum numbers of this picture.

To obtain such a two-phased system, we start with a disc at $\nu = 1/3$, add an auxiliary layer to region II and condense the appropriate boson present in this system. First we need to find the quantum groups that label the excitations of the system. Looking at the CFT of the Laughlin state, the vertex operators that insert an electron and a fundamental quasihole are

$$V_e(z_i) = e^{i\sqrt{3}\phi(z_i)} \tag{5.3}$$

$$V_{qh_0}(u_i) = e^{i\frac{1}{\sqrt{3}}\phi(u_i)} \tag{5.4}$$

The electron has charge e from which it follows that the quasihole has charge $Q_{qh_0} = e/3$ and the spins of the fields are the same as their conformal dimensions. For a TQFT description we only keep sectors modulo two times the electron. From this it follows that region I is described by a $\mathbb{Z}_6$ theory. The different excitations carry a label a corresponding to the irreps of this symmetry, i.e. $a \in \mathbb{Z}_6$. The electric charges, topological spins and quantum dimensions of the spectrum are

$$Q_a = \frac{ea}{3}, \qquad h_a = \frac{a^2}{6}, \qquad d_a = 1 \tag{5.5}$$

Evidently, the electron is labeled by 3 and the fundamental quasihole by 1. Note that all the sectors have unit quantum dimension, since this is an Abelian theory.

Building up the system we have $\mathcal{A}_0 = \mathbb{Z}_6$ in region I and as auxiliary (smaller) disc we choose $\mathbb{Z}_{30}$ which results in $\mathcal{A}_1 = \mathbb{Z}_6 \times \mathbb{Z}_{30}$ in region II. There are more than one non-trivial bosons in $\mathcal{A}_1$, but we only let $B_1 = (1, 5)$ condense. That this is indeed a boson follows from the fact that

$$d_{(1,5)} = 1, \qquad h_{(1,5)} = \frac{1}{6} + \frac{5^2}{30} \in \mathbb{Z} \tag{5.6}$$

When the condensate forms, the initial symmetry is broken and is replaced by a smaller symmetry. In practice, we should look at the fusion rules of all the sectors that were present in $\mathcal{A}_1$ with this condensate. Since $(1,5)$ is a simple current of order 6 and all sectors have quantum dimensions equal to unity, none of the sectors will split and orbits under fusion with the condensate consist of six sectors which become identified with each other. For $a \in \mathbb{Z}_6$ and $b \in \mathbb{Z}_{30}$ this can be expressed as

$$(a,b) \sim (a+q, b+5q), \quad \text{for } q = 0, ..., 5 \tag{5.7}$$

To find the broken phase a representative must be chosen from every orbit. A convenient choice turns out to be

$$\mathcal{T}_1 = \{(0,a) : a \in \mathbb{Z}_{30}\} \tag{5.8}$$

These sectors are the excitations of the broken phase in region II. They obey good fusion rules, but consistent braiding has not been considered so far. In order to find which sectors braid non-trivially with the condensate and thus become confined, we need to look at the spins of the lifts of each sector $(0,a) \in \mathcal{T}$. From (5.7) it is clear that the lifts of a general sector $(0,a)$ are $(q, a+5q)$ for $q = 0, ..., 5$. All these lifts should have the same spin factor in order to have consistent braiding with the condensed sector. The difference in spin of the lifts is

$$h_{\text{dif}} = \frac{a^2}{30} - \frac{q^2}{6} - \frac{(a+5q)^2}{30} = -q^2 - \frac{aq}{3} \tag{5.9}$$

Whenever this difference is an integer the lifts have equal spin factors. Explicitly this means that the sectors $(0,a)$ that are unconfined must have $a \in 3\mathbb{Z}$. After expelling all confined excitations from the bulk of region II, we are left with a broken unconfined phase that has excitations labeled by

$$\mathcal{U}_1 = \{(0,3b) : b = 0, 1, ..., 9\} \tag{5.10}$$

These sectors form a closed set under fusion and have good braiding statistics. The spins of the sectors in region II are

$$h_b = \frac{3b^2}{10} \tag{5.11}$$

$\mathcal{A}_0$	$\mathcal{T}_1$	$\mathcal{U}_1$	$\mathcal{A}_0$	$\mathcal{T}_1$	$\mathcal{U}_1$
$(0,0)$	$(0,0)$	$(0,0)$	$(3,0)$	$(0,15)$	$(0,15)$
	$(0,3)$	$(0,3)$		$(0,18)$	$(0,18)$
$(5,0)$	$(0,5)$		$(2,0)$	$(0,20)$	
	$(0,6)$	$(0,6)$		$(0,21)$	$(0,21)$
	$(0,9)$	$(0,9)$		$(0,24)$	$(0,24)$
$(4,0)$	$(0,10)$		$(1,0)$	$(0,25)$	
	$(0,12)$	$(0,12)$		$(0,27)$	$(0,27)$

Table 5.2: *The excitations in region I and II can be expressed as sectors of $\mathcal{T}_1$. All the sectors of $\mathcal{T}_1$ that are not listed in this table are confined to the boundary between the two regions. We see that there is one non-trivial excitation that can move through the wall between both regions, which is $(0,15)$ and has unit electric charge.*

Therefore, the fundamental quasihole in region II, q_1 has spin $h_{q_1} = \frac{3}{10}$. As for the electric charge, we know that $(3,0)$ has charge e. To find the charge of the fundamental quasihole in region II we need to compare it to $(3,0)$. This can be done by fusing the quasihole five times with itself and then fusing it three times with the boson B_1, i.e. $(0,3)^{\times 5} = (0,15) \sim (3,0)$. Since electric charge adds under fusion it should be clear that the fundamental quasihole has charge $Q_{q_1} = \frac{e}{5}$. This charge and statistics fully agree with the predictions of Haldane and Halperin [14, 15].

This is the point where we have realized a configuration as in Fig. 3.2 where region I is a FQH state at filling fraction $\nu_I = 1/3$ with excitations given by $\mathcal{A}_0$ and region II has $\nu_{II} = 2/5$ with excitations (5.10). The excitations in both regions can be expressed as sectors of $\mathcal{T}_1$, which is shown in Tab. 5.2. Now we have a description of what processes are possible in each region and on the domain wall between the two regions.

Let us take a closer look at this wall. There is one non-trivial excitation that can move into both regions, which means it can travel through the wall. This sector is labeled by $(0,15)$ in region II and by $(3,0)$ in region I. We recognize this excitation as the electron. Furthermore, the fundamental excitation confined to the wall has charge $e/15$.

The authors of Ref. [46] consider a setup with a quantum Hall droplet at filling fraction ν_d that is surrounded by a quantum Hall fluid at $\nu_s \neq \nu_d$. There are two point contacts where tunneling between the ν_s edges can occur and there is tunneling between the ν_s edge and the edge of the droplet, see Fig. 5.1. They charge the droplet by adding flux to it. This leads to a certain periodicity of the ground state energy and radius of the droplet,

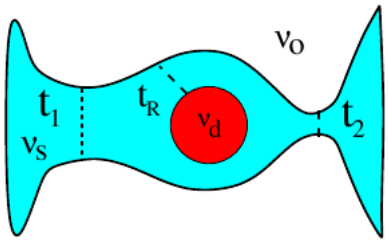

Figure 5.1: *A system with quantum Hall states at three different filling fractions ν_i. Flux is adiabatically inserted in the droplet leading to periodicities in the ground state energy and the radius of the droplet. Figure taken from Ref. [46].*

which depends on the different filling fractions. As an example they focus on $\nu_d = 2/5$, $\nu_s = 1/3$, and $\nu_0 = 0$, i.e. the case we just discussed. What they find on the inner edge is a Laughlin state at $\nu = 1/15$. This agrees with our results, since the fundamental excitation we find is $(0, 1)$, which has a charge $e/15$.

Let us briefly sketch how they obtain their results of this specific case. The idea is that inserting a flux quantum in the droplet will bind a charge of $2e/5$. This charge must come from the other regions, so $e/15$ comes from the inner edge and $e/3$ from the outer edge. Leading to negative charging of the two edges every time that flux is inserted. Since the outer edge can act as a reservoir it takes a period of $5\Phi_0$ to reach the initial situation of neutral edges. This period coincides with the measurements of Camino et al. that were mentioned in subsection 2.2.3. Nevertheless, the authors of Ref. [46] have a different interpretation of this period than Camino et al. They explain the predicted period by charging of the edges instead of a result of the statistics of the quasiparticles.

This was a first example of a phase transition between two FQH states belonging to the same hierarchy. We considered two states from the HH hierarchy, which are Abelian states. Now we move on to the next example which will be somewhat different, since it deals with non-Abelian states.

5.2.2 BS hierarchy at $\nu_I = \frac{5}{2}$ and $\nu_{II} = \frac{12}{5}$

This subsection will be on an explicit example of the BS hierarchy, which aims at describing the FQH effect in the second Landau level. We want to induce a phase transition between the MR state at $\nu = 5/2$ and the

next level of the BS hierarchy which has filling fraction $\nu = 12/5$. This state is obtained by letting the quasiholes of the MR state favor the vacuum channel.[1] These states are of particular interest for TQC. Even though the MR state allows for TQC, it is not universal. Other states have been proposed for $\nu = 12/5$. One of these is the Read-Rezayi state at $k = 3$ [17] which has a Fibonacci structure and thus allows for universal quantum computation. If the BS hierarchy turns out to be the right description of the state at $\nu = 12/5$ it would mean that it does not allow for universal quantum computation, since the non-Abelian part would be the same as for the MR state. The authors of Ref. [47] present numerical data where they compare the RR and BS state as well as the Abelian HH state at $\nu = 12/5$. Neither of these states can be ruled out so far.

Having said this, we proceed with topological symmetry breaking to go from the MR state to the next level of the BS hierarchy. Again we will use an auxiliary layer to obtain the desired phase in region II. First start with the MR state as the zeroth level of hierarchy. In previous parts of this thesis only the non-Abelian part of MR was included in the breaking scheme. Since the hierarchization of Bonderson and Slingerland happens in the $U(1)$ part only, this alters our previous approach in some sense.

First go back to the CFT of the MR state. It has the following spectrum

$$\mathcal{C}_0 = \{(I, n), (\psi, n), (\sigma, n + \frac{1}{2}) : n \in \mathbb{Z}\} \tag{5.12}$$

Instead of using the full CFT we choose a description in terms of a TQFT. This means we will not consider infinitely many sectors. The excitations in region I can now be written as representations of the quantum group

$$\mathcal{A}_0 = Ising \otimes \mathbb{Z}_4 \tag{5.13}$$

Note that the excitations with σ in the Ising sector are elements of Ising $\otimes$ $(\mathbb{Z}_4 + \frac{1}{2})$, but we will not be mentioning this explicitly throughout. As auxiliary layer we choose $\overline{\mathbb{Z}}_{20}$, which leads to an unbroken phase in region II described by

$$\mathcal{A}_1 = Ising \otimes \mathbb{Z}_4 \otimes \overline{\mathbb{Z}}_{20} \tag{5.14}$$

[1] If instead quasiparticles pair into the vacuum channel, the first level of the BS hierarchy would have $\nu = 8/3$.

The quantum dimension and spin of these sectors are

$$d_{(a_I,a,b)} = d_{a_I}, \qquad h_{(a_I,a,b)} = h_{a_I} + \frac{a^2}{4} - \frac{b^2}{20} \tag{5.15}$$

The electron, e_0, fundamental quasihole, qh_0 and a boson, B_1 can be written as

$$e_0 = (\psi, 2, 0) \tag{5.16}$$
$$qh_0 = (\sigma, \tfrac{1}{2}, \tfrac{1}{2}) \tag{5.17}$$
$$B_1 = (I, 1, 5) \tag{5.18}$$

The boson B_1 is the one that needs to be condensed to get to the next level of the hierarchy. Since the boson is trivial in the Ising sector we only need to consider the $U(1)$ part of the theory, as was mentioned before. The Ising sectors can be put back in at any time. For simplicity we will not write the half integer values of the excitations corresponding to the σ Ising sector. Again this can be put back in at any time.

When B_1 forms a condensate, the sectors of $\mathcal{A}_1$ will form orbits under fusion with it that have a length of four sectors. Choosing a representative from each orbit the broken phase in region II has an underlying symmetry

$$\mathcal{T}_1 = \{(0, a) : a \in \overline{\mathbb{Z}}_{20}\} \tag{5.19}$$

To find which fields become confined and which are unconfined, we need to look at the spin factors of the lifts of the fields belonging to $\mathcal{T}_1$. An arbitrary orbit can be written as $(0, a) \sim (q, a + 5q)$, where $q = 0, 1, 2, 3$. The difference in spin between those fields is

$$h_{\text{dif}} = \frac{-a^2}{20} - \frac{q^2}{4} + \frac{(a+5q)^2}{20} = q^2 + \frac{aq}{2} \tag{5.20}$$

If $h_{\text{dif}} \in \mathbb{Z}$ then the fields have the same spin factor and are unconfined. We see that the fields $(0, a)$ which have $a \in 2\mathbb{Z}$ satisfy this condition. These fields will form the broken unconfined phase of region II described by

$$\mathcal{U}_1 = \{(0, 2a) : a = 0, 1, ..., 9\} \subset \overline{\mathbb{Z}}_{20} \tag{5.21}$$

The topological spectrum of this new phase is

$$Ising \otimes \mathcal{U}_1 = \{(I, n), (\psi, n), (\sigma, n + \frac{1}{2}) : n \in \mathcal{U}_1\} \tag{5.22}$$

That this spectrum is indeed closed under fusion might not be clear at first sight, because of the half integral values corresponding to σ. To see that it is indeed closed, let us fuse two arbitrary quasiholes with each other:

$$\begin{aligned} (\sigma, \frac{1}{2}, 2a + \frac{1}{2}) \times (\sigma, \frac{1}{2}, 2a' + \frac{1}{2}) &= (1/\psi, 1, 2(a + a') + 1) \\ &\sim (1/\psi, 0, 2(a + a') + 16) \end{aligned} \tag{5.23}$$

which is clearly in $Ising \otimes \mathcal{U}_1$. Furthermore, it can be shown that the spectrum in (5.22) is generated by two fundamental excitations: $q_1 = (I, 0, 2)$ and $qh_1(\sigma, \frac{1}{2}, \frac{9}{2})$.

We accomplished to describe a two-phased system where the excitations in region I are labeled by $\mathcal{A}_0$ and in region II by $Ising \otimes \mathcal{U}_1$, which have a wall between them described by $Ising \otimes \mathcal{T}_1$.

Braiding and electric charges In order to compare this result to those of Ref. [42], we look at the predicted electric charge and spin of the fundamental excitations in region II[2]

$$h_{q_1} = -\frac{2^2}{20} = -\frac{1}{5} \tag{5.24}$$

$$h_{qh_1} = \frac{(1/2)^2}{4} - \frac{(9/2)^2}{20} = -\frac{19}{20} \tag{5.25}$$

The charge of these excitations can also be calculated. This is done by noting that the electron $(\psi, 2, 0)$ has charge e, which solely comes from the $U(1)$ part $(2, 0)$. Fusing q_1 five times with itself is equivalent to the electron, i.e. $(0, 2)^{\times 5} = (0, 10) \sim (2, 0)$. This implies that q_1 must have charge $e/5$. To calculate the charge of qh_1 note that $(0, 4)$ which has charge $2e/5$ can split into two qh_1 particles

[2] For qh_1 we only consider the spin of the Abelian part. The σ sector gives an additional factor of $1/16$.

$$(0,4) \sim (1,9) \to (\tfrac{1}{2},\tfrac{9}{2}) \times (\tfrac{1}{2},\tfrac{9}{2}) \tag{5.26}$$

From this it follows that qh_1 also has charge $e/5$. The charges of all the other excitations in (5.22) can be found by noticing that electric charges add under fusion. As an exercise let us check that q_1 is indeed fundamental, i.e. it cannot split into two other excitations.

$$(I,0,2) \sim (I,1,7) \to (\sigma,\tfrac{1}{2},\tfrac{7}{2}) \times (\sigma,\tfrac{1}{2},\tfrac{7}{2}) \tag{5.27}$$

since $(\sigma,\frac{1}{2},\frac{7}{2})$ is confined in region II, q_1 cannot split into two bulk excitations. Both the spin and charge that we find are the same as predicted in Ref. [42].

Wall excitations Let us focus on the wall between the two phases. Not all of the fields in $\mathcal{T}_1$ will stay on this wall. For convenience we drop the Ising sectors and factors of $1/2$ for the moment. The fields in the $\mathcal{A}_0$ phase can be rewritten in terms of $\mathcal{T}_1$ fields as

$$(0,0) \sim (0,0) \tag{5.28}$$
$$(1,0) \sim (0,15) \tag{5.29}$$
$$(2,0) \sim (0,10) \tag{5.30}$$
$$(3,0) \sim (0,5) \tag{5.31}$$

Those four fields can move from the wall into the bulk of region I. The fields $(0,2a)$ with $a = 0,1,...,9$ can move from the wall into region II. The correspondence between the bulk excitations and the fields of $\mathcal{T}_1$ is listed in Tab. 5.3. All the $\mathcal{T}_1$ fields that are not listed in this table are strictly confined to the wall. Notice that there is one non-trivial excitation which can move from region I to region II through the wall. This is the field $(0,10)$, which is equivalent to $(2,0)$ and has unit electric charge. Furthermore, the excitation with smallest electric charge that is strictly confined to the wall is $(0,1)$ and it has charge $Q_{(0,1)} = e/10$.

This concludes the section where two examples of a transition between hierarchical phases were presented. Next, we would like to show how a general HH and BS hierarchy can be constructed by Bose condensation.

$\mathbb{Z}_4$	$\mathcal{T}$	$\mathcal{U}$	$\mathbb{Z}_4$	$\mathcal{T}$	$\mathcal{U}$
$(0,0)$	$(0,0)$	$(0,0)$	$(2,0)$	$(0,10)$	$(0,10)$
	$(0,2)$	$(0,2)$		$(0,12)$	$(0,12)$
	$(0,4)$	$(0,4)$		$(0,14)$	$(0,14)$
$(3,0)$	$(0,5)$		$(1,0)$	$(0,15)$	
	$(0,6)$	$(0,6)$		$(0,16)$	$(0,16)$
	$(0,8)$	$(0,8)$		$(0,18)$	$(0,18)$

Table 5.3: *The fields present in the bulk of region I and II are listed in the $\mathbb{Z}_4$ and $\mathcal{U}_1$ column respectively. The $\mathcal{T}_1$ field corresponding to each of the bulk fields is shown in the same row. There is one non-trivial field that can be present in both phases and it has unit electric charge.*

5.3 General hierarchy picture

This section is concerned with a more general description of phase transitions between different levels of a hierarchy. First we will consider such a transition between an arbitrary 0^{th} and 1^{st} level of the HH hierarchy. Once we have obtained this we can consider phase transitions between an arbitrary number of levels of the HH hierarchy. Finally, we will use these results to also obtain the BS hierarchy for arbitrary levels. The derivations in this section will lean upon the K-matrix formalism, which allows for compact notation.

5.3.1 Arbitrary K-matrix at 1^{st} level of HH hierarchy

We start with the HH hierarchy where the 0^{th} level is at filling fraction $\nu = 1/m_0$, for m_0 odd. This is an arbitrary Laughlin state. The vertex operators corresponding to the insertion of an electron and fundamental quasihole are

$$V_{e_0} = e^{i\sqrt{m_0}\phi_0} \tag{5.32}$$

$$V_{q_0} = e^{i\frac{1}{\sqrt{m_0}}\phi_0} \tag{5.33}$$

This tells us that the 0^{th} level is described by the quantum group

$$\mathcal{A}_0 = \mathbb{Z}_{2m_0} \tag{5.34}$$

which labels the spectrum of region I. Since we are dealing with just one level so far the K-matrix is just a number: $K_{00} = m_0$. To get to the 1st level of the hierarchy $\mathbb{Z}_{2m_0}$ needs to be tensored with an appropriate theory and a bosonic field should be condensed. We know that the state at the next level has K-matrix

$$K = \begin{pmatrix} K_{00} & K_{01} \\ K_{10} & K_{11} \end{pmatrix} \tag{5.35}$$

with $K_{00} = m_0$ odd, K_{11} even, and $K_{01} = K_{10} = -\text{sgn}(K_{11})$.

It turns out that we should use $\mathbb{Z}_{2m_1m_0^2}$ as an auxiliary layer in region II, where $m_{i>0} = K_{ii} - \frac{1}{m_{i-1}}$. This choice leads to an unbroken phase in region II described by

$$\mathcal{A}_1 = \mathbb{Z}_{2m_0} \otimes \mathbb{Z}_{2m_1m_0^2} \tag{5.36}$$

The bosonic sector that forms the condensate is $(K_{01}, |m_1m_0|)$. This is indeed a boson since it has spin

$$h_{B_1} = \frac{1}{2m_0} + \frac{{m_1}^2{m_0}^2}{2m_1{m_0}^2} = \frac{1}{2m_0} + \frac{m_1}{2} = \frac{K_{11}}{2} \tag{5.37}$$

which is an integer because $K_{11} \in 2\mathbb{Z}$ and it has quantum dimensions equal to 1. The sectors of $\mathcal{A}_1$ form orbits under fusion with B_1. Such an orbit has length $2m_0$. After the appropriate identifications we reach the broken $\mathcal{T}_1$-theory, which is given by

$$\mathcal{T}_1 = \{(0, a) : a \in \mathbb{Z}_{2m_1m_0^2}\} \tag{5.38}$$

Some of these $\mathcal{T}_1$ sectors must become confined. In order to see which, we need to look at the difference in spin of sectors that belong to the same orbit. Any orbit can be written as

$$(0, a) \sim (K_{01}q, a + |m_1m_0|q) \tag{5.39}$$

where $q = 0, 1, ..., 2m_0 - 1$. The difference in spin of $(0, a)$ with an arbitrary lift $(K_{01}q, a + |m_1m_0|q)$ is

$$\begin{aligned} h_{\text{dif}} &= \frac{a^2}{2m_1{m_0}^2} - \frac{(K_{01}q)^2}{2m_0} - \frac{(a+|m_1m_0|q)^2}{2m_1{m_0}^2} \\ &= -\frac{q^2}{2}(\frac{1}{m_0}+m_1) - \frac{q|m_1|a}{m_1m_0} \end{aligned} \tag{5.40}$$

Whenever $h_{\text{dif}} \in \mathbb{Z}$ then $(0,a)$ is unconfined. Since the first term of (5.40) is an integer, this results in

$$(0,a) \text{ unconfined} \Leftrightarrow a \in m_0\mathbb{Z} \tag{5.41}$$

After the confined fields are driven out of the bulk of region II the unconfined broken phase becomes

$$\mathcal{U}_1 = \{(0,m_0b) : b = 0,1,...,2|m_1m_0|-1\} \subset \mathbb{Z}_{2m_1m_0^2} \tag{5.42}$$

Finally, this results in a configuration with region I described by $\mathcal{A}_0$ and region II by $\mathcal{U}_1$. These phases are separated by a wall $\mathcal{T}_1$. Next, we want to consider the possible boundary processes and see what quantum numbers can be associated to the excitations of region II. These must be compared to the numbers that follow directly from the K-matrix.

Wall excitations The excitations that can move freely in region I are given by $(a,0) \sim (0,a|m_1m_0|)$, where $a \in \mathbb{Z}_{2m_0}$. In region II the fields $(0,bm_0)$, for $b = 0,1,...,2|m_1m_0|-1$ can move from the wall into the bulk. All the other $\mathcal{T}_1$ fields are strictly confined to the wall between both regions.

There is also a possibility for some fields to move through the wall from one region to the other. In order to find those fields, note that we have to demand

$$(0,a|m_1m_0|) = (0,bm_0) \tag{5.43}$$

This implies that these fields must have $a = m_0\mathbb{Z}$. Since $a \in \mathbb{Z}_{2m_0}$ there are only two values that meet this requirement, namely $a \in \{0,m_0\}$. So the two fields that can move freely on the entire disc are $(0,0)$ and $(0,|m_1|m_0^2)$, the latter being equivalent to $(m_0,0)$, which has unit electric charge.

The fundamental excitation that is strictly confined to the wall is $(0,1)$ and it has electric charge $Q_{(0,1)} = \frac{e}{|m_1 m_0^2|}$.

Braiding and electric charge Let us consider the spin and electric charge of the fields in the $\mathcal{U}_1$-algebra and compare them with the results from the K-matrix. The spins of these fields are

$$h_b = \frac{(m_0 b)^2}{2m_1 {m_0}^2} = \frac{b^2}{2m_1} \tag{5.44}$$

The spin obtained for the fundamental quasihole from the K-matrix formalism where $\hat{t}_i = \delta_{ji}$ is

$$h_{q_1} = \frac{1}{2}\hat{t}_1^\dagger \cdot K^{-1} \cdot \hat{t}_1 = \frac{K_{00}}{2\mathrm{det}K} = \frac{m_0}{2(K_{00}K_{11} - 1)} = \frac{1}{2m_1} \tag{5.45}$$

All excitations can be reached under fusion of the fundamental quasihole with itself. So the spin of an excitation nq_1 is $h_{nq_1} = \frac{n^2}{2m_1}$, which is the same as the spins obtained from the condensation process.

The electric charge of q_1 can be found by comparing it to the electron $e_0 = (m_0, 0)$, which is equivalent to $(0, m_0|m_1 m_0|)$. On the other hand, if we fuse the quasihole $|m_1 m_0|$ times with itself we also get $(0, m_0|m_1 m_0|)$. This means that it must have charge $Q_{q_1} = \frac{e}{|m_1 m_0|}$.

The electric charge obtained from the K-matrix formalism is given by

$$Q_{q_1} = e\hat{t}_0^\dagger \cdot K^{-1} \cdot \hat{t}_1 = \frac{-eK_{01}}{\mathrm{det}K} = \frac{-eK_{01}}{m_1 m_0} = \frac{e\mathrm{sgn}(m_1)}{m_1 m_0} = \frac{e}{|m_1 m_0|} \tag{5.46}$$

which agrees with our results. Since any excitation can be reached by fusing q_1 an appropriate number of times with itself, the electric charge of an arbitrary excitation in region II is

$$Q_{nq_1} = \frac{ne}{|m_1 m_0|} \tag{5.47}$$

Here we want to conclude this subsection by mentioning that the results obtained in subsection 5.2.1 are recovered by plugging in $K_{00} = 3$ and $K_{11} = 2$.

5.3.2 Arbitrary K-matrix at k^{th} level of HH hierarchy

The above strategy can be repeated k times which will lead to the k^{th} level of the HH hierarchy. All the information that is needed is contained in the K-matrix. In the following we will sketch how this works and give general formulae for this breaking process. Recall that the K-matrix has nonzero entries: K_{00} odd, K_{jj} even for $j > 0$, and $K_{j,j+1} = K_{j+1,j} = -\text{sgn}(K_{j+1,j+1})$.

The 0^{th} level is again described by $\mathcal{A}_0 = \mathbb{Z}_{2m_0}$. To obtain k levels on top of $\mathcal{A}_0$ we should start with k auxiliary layers:

$$\mathcal{A}_k = \mathbb{Z}_{2m_0} \otimes \mathbb{Z}_{2m_1 m_0^2} \otimes ... \otimes \mathbb{Z}_{2m_k m_{k-1}^2 ... m_0^2} \tag{5.48}$$

Note that we use $\mathcal{A}_k$ to describe all regions. The way to look at this is that in the outermost region we have $\mathcal{A}_0 = \mathbb{Z}_{2m_0} \otimes \{0\} \otimes ... \otimes \{0\} \subset \mathcal{A}_k$. Even though only the $\mathcal{A}_0$ labels are present in the outermost region an excitation also carries the trivial label from all other regions. To induce phase transitions between the k regions the following k bosons need to form condensates

$$B_j = (\underbrace{0, 0, ..., 0}_{j-1 \text{ times}}, -\text{sgn}(m_{j-1}m_j)|m_{j-2}...m_0|, |m_j m_{j-1}...m_0|, \underbrace{0, ..., 0}_{k-j \text{ times}})$$

If the bosons condense one by one it will lead to k phase transitions where the broken unconfined theories are $\mathcal{A}_0$ and

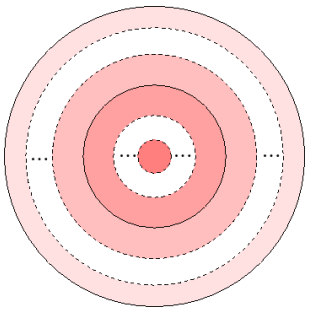

Figure 5.2: *Building a hierarchy of k levels. The outermost region is the 0^{th} level of the hierarchy, going inwards means moving up in the hierarchy. Finally the inner region is the k^{th} level. Note that there are k boundaries in this configuration.*

$$\mathcal{U}_j = \{(\underbrace{0,...,0}_{j \text{ times}}, |m_{j-1}...m_0|b, \underbrace{0,...,0}_{k-j \text{ times}}) : b = 0,1,...,2|m_j...m_0| - 1\} \quad (5.49)$$

for $j = 1, 2, ..., k$. There are k walls between those phases, namely

$$\mathcal{T}_j = \{(\underbrace{0,...,0}_{j \text{ times}}, a, \underbrace{0,...,0}_{k-j \text{ times}}) : a \in \mathbb{Z}_{2m_j m_{j-1}^2...m_0^2}\} \quad (5.50)$$

Wall excitations To see which of the $\mathcal{T}_j$ fields can move into the bulk of the two regions which it separates, the fields of the outer region described by $\mathcal{U}_{j-1}$ need to be rewritten explicitly. The fields of $\mathcal{U}_j$ living in the inner region are already in the same form as the $\mathcal{T}_j$ fields. To write the $\mathcal{U}_{j-1}$ fields in the same form as $\mathcal{T}_j$ we need to fuse it $\pm b$ times with the boson B_j depending on the sign of $m_{j-1}m_j$. This results in

$$(\underbrace{0,...,0}_{j-1 \text{ times}}, b, \underbrace{0,...,0)}_{k-j+1 \text{ times}} \sim (\underbrace{0,...,0}_{j \text{ times}}, \text{sgn}(m_{j-1}m_j)b|m_j...m_0|, \underbrace{0,...,0}_{k-j \text{ times}}) \quad (5.51)$$

These fields can move from the wall into the outer region and the ones in (5.49) can move into the inner region. All the other $\mathcal{T}_j$ excitations will be strictly confined to the $\mathcal{U}_{j-1}/\mathcal{U}_j$ wall. The smallest $\mathcal{T}_j$ excitation is confined and has charge $e/|m_j m_{j-1}^2...m_0^2|$.

Braiding and electric charge The spins of the excitations present in the j^{th} level, for $j = 1, ..., k$ are given by

$$h_b = \frac{(|m_j...m_0|b)^2}{2m_j m_{j-1}^2...m_0^2} = \frac{b^2}{2m_j} \quad (5.52)$$

To calculate the spins directly from the K-matrix, first note that in regions for $j < k$ we should not use the whole K-matrix. As in the discussion under (5.48), we used an artificial way to write the auxiliary layers also in the regions where they are not present. The K-matrix should not notice these artificial layers. Hence, let us define $K^{(j)}$ as the first $j \times j$ block of the full K-matrix. This enables us to calculate the spins and electric charges for

every level $j = 1, ..., k$ directly from the K-matrix so that it can be compared to our results. The spin of the fundamental quasihole at level j is

$$h_{q_j} = \frac{1}{2}\hat{t}_j^{\dagger} \cdot (K^{(j)})^{-1} \cdot \hat{t}_j = \frac{1}{2}[(K^{(j)})^{-1}]_{jj} = \frac{\det K^{(j-1)}}{2\det K^{(j)}} = \frac{1}{2m_j} \tag{5.53}$$

For an arbitrary excitation in the j^{th} level the spin is given by $h_{nq_j} = \frac{n^2}{2m_j}$. These are the same spins as found in (5.52).

The electric charges for the fields in $\mathcal{U}_j$ can be found by comparing the fundamental excitation, q_j to the electron, e_0. It can be shown that the $\mathcal{U}_j$ field that is equivalent to the electron is

$$e_0 \sim (\underbrace{0, ..., 0}_{j \text{ times}}, |m_j m_{j-1}^2 ... m_0^2|, \underbrace{0, ..., 0}_{k-j \text{ times}}) \tag{5.54}$$

Since the fundamental excitation is

$$q_j = (\underbrace{0, ..., 0}_{j \text{ times}}, |m_{j-1} ... m_0|, \underbrace{0, ..., 0}_{k-j \text{ times}}) \tag{5.55}$$

it must fuse $|m_j ... m_0|$ times with itself in order to be equal to (5.54). This means that the charge of q_j is given by $e/|m_j ... m_0|$ and any other excitation labeled by b from (5.49) is

$$Q_{bq_j} = \frac{eb}{|m_j ... m_0|} \tag{5.56}$$

Again, compare this with the electric charge of the fundamental excitation obtained from the K-matrix formalism

$$\begin{aligned} Q_{q_j} &= e\hat{t}_0^{\dagger} \cdot (K^{(j)})^{-1} \cdot \hat{t}_j = e\frac{(-1)^j K_{j-1,j} ... K_{12} K_{01}}{\det K^{(j)}} \\ &= e\frac{(-1)^j (-1)^j \text{sgn}(m_j ... m_1)}{m_j ... m_0} = \frac{e}{|m_j ... m_0|} \end{aligned} \tag{5.57}$$

Clearly, the electric charges from both approaches are in agreement once again.

Let us end this subsection on the HH hierarchy by mentioning that the spins and electric charges agree with the special cases treated in subsection 5.2.1 and 5.3.1.

5.3.3 BS hierarchy on MR state

In subsection 5.2.2 we presented an example of the BS hierarchy, where one level was built on the MR state. Now we can do this for an arbitrary number of levels. This follows from the fact that the BS hierarchy is only built in the Abelian part of the MR state, enabling us to use the K-matrix as before. What is different is that we must choose $K_{00} = m_0 = 2$ instead of odd, if we want to build a hierarchy on the MR state.[3]

With this subtlety in mind we can copy the results of the previous subsection and directly move on to the theories that describe the broken unconfined phases at each level of the BS hierarchy. The charge spectrum of each phase for $j = 1, 2, ..., k$ is

$$Ising \otimes \mathcal{U}_j = \{(I, n), (\psi, n), (\sigma, n + \frac{1}{2}) : n \in \mathcal{U}_j\} \tag{5.58}$$

where $\mathcal{U}_j$ is given in (5.49).

Wall excitations Once more let us consider the wall excitations. In this case there are k different walls and the theory that describes all possible fields on each wall for $j = 1, 2, ..., k$ is

$$Ising \otimes \mathcal{T}_j = \{(I, n), (\psi, n), (\sigma, n + \frac{1}{2}) : n \in \mathcal{T}_j\} \tag{5.59}$$

Not all of these fields are strictly confined to the wall. We have to determine which fields can move into the bulk of one or both of the two adjacent regions. The fields that can move into the bulk of the inner region are given in (5.58) which is a subset of $Ising \otimes \mathcal{T}_j$. To find the fields that can move into the bulk of the outer region we need to rewrite the fields in $Ising \otimes \mathcal{U}_{j-1}$ somewhat in

[3] The quasiholes of the MR state could also choose to fuse to the ψ channel. When this is the case $K_{00} = 1$ [42].

order to match them with the fields in $Ising \otimes \mathcal{T}_j$. An arbitrary excitation, with $b \in \mathcal{U}_{j-1}$, can be written as

$$\begin{array}{rcl} (I/\psi, \overbrace{0,...,0}^{j-1 \text{ times}}, b, \overbrace{0,...,0)}^{k-j+1 \text{ times}} & \sim & (I/\psi, \overbrace{0,...,0}^{j \text{ times}}, pb|m_j...m_0|, \overbrace{0,...,0)}^{k-j \text{ times}} \\ (\sigma, \underbrace{\tfrac{1}{2},...,\tfrac{1}{2}}_{j-1 \text{ times}}, b+\tfrac{1}{2}, \underbrace{\tfrac{1}{2},...,\tfrac{1}{2})}_{k-j+1 \text{ times}} & \sim & (\sigma, \underbrace{\tfrac{1}{2},...,\tfrac{1}{2}}_{j \text{ times}}, pb|m_j...m_0|+\tfrac{1}{2}, \underbrace{\tfrac{1}{2},...,\tfrac{1}{2})}_{k-j \text{ times}} \end{array} \tag{5.60}$$

where $p = \text{sgn}(m_{j-1}m_j)$. These fields can move into the bulk of the outer region.

The spins of the fields with I or ψ are the same as those given in (5.52) where 1/2 has to be added for ψ. The charges for those fields are shown in (5.56). For the σ fields future work is needed to find a general formula for spins and charges.

In this chapter it has been shown that topological symmetry breaking can be used to describe phase transitions between different levels of the hierarchy picture. This picture is a way to generate FQH states building them on top of some initial parent state. In this way all observed filling fractions can be covered. Usually these hierarchy pictures give wavefunctions for the different states. In general, it is difficult to find analytic wavefunctions or even numerical ones. Therefore, we tried to reconstruct a hierarchy by applying topological symmetry breaking. For this we do not need wavefunctions, just the excitation spectrum with the appropriate quantum numbers is needed.

Explicitly, we have considered the HH and BS hierarchy. The former being a hierarchy of Abelian states building on a Laughlin state and the latter a non-Abelian hierarchy building on the MR state where all the daughter states have the same non-Abelian sectors as the MR state. After presenting two explicit examples of both hierarchies, we showed how to obtain topological spectra for an arbitrary number of levels as well as expressions for the excitations on the boundary between two adjacent regions. The spins and electric charges are in agreement with what is found in the literature. The

only difficulty that remains is obtaining generalized expressions of spins and charges for the sectors that contain σ for the BS hierarchy with k arbitrary levels.

Besides this challenge there are some more questions that we would like to answer. What we have not done yet is try to reproduce other hierarchies, such as those proposed by Hermanns and Levin-Halperin which were briefly touched upon in the first section of this chapter.

Furthermore, it would be interesting to write down wavefunctions from the spectra we find. This can be done by writing vertex operators for the different excitations and taking correlators of these operators. The difficulty in this is that we need to go from a TQFT to a CFT. At first sight there seems to be some ambiguity in the fact that for the TQFT description we are dealing with a finite number of sectors, but these become infinite when the CFT is considered.

Moreover, Wen has formulated the edge properties of FQH states in terms of the K-matrix [48]. It would be interesting to compare the spectrum of edge excitations we find to his results.

Lastly, there is a possibility that the quasiholes in the zeroth level of the BS hierarchy pair up into the ψ fusion channel as was mentioned in a footnote in subsection 5.3.3. This should not lead to too much difficulty since it seems that the only difference is that the K_{11} should be chosen odd instead of even [42]. Probably this leads to the same expressions as found in subsection 5.3.3, but we have not yet tested this explicitly.

CHAPTER 6

Conclusions and outlook

This final chapter offers some conclusions with respect to the results obtained and gives an outlook on interesting projects for future work.

We have applied topological symmetry breaking to different FQH states. In order to do this, we introduced the main concepts of planar physics in chapter 2. Here we saw how (non-)Abelian anyons arise naturally considering the quantum statistics of particles in 2D. These anyons carry quantum numbers associated to fusing and rotating the particles. Also FQH fluids have been discussed, since these are real physical systems that exhibit topological phases and can carry anyonic excitations. A nice application of particles with non-Abelian anyonic statistics is TQC. We showed that a qubit can be encoded in a set of anyons and how it can be manipulated by braiding anyons around each other.

In chapter 3 the different steps of topological symmetry breaking have been presented. Starting with a topological phase, its excitations are labeled by irreps of a quantum group describing the underlying symmetry of the system. If there is a bosonic excitation in the spectrum and it condenses, the initial symmetry is broken. The excitations rearrange themselves where some may become confined. Eventually, we reach a phase with an excitation spectrum described by a different quantum group. Most importantly, this method naturally provides a description of the domain wall between the two

phases.

In the second part of this thesis we have applied topological symmetry breaking to several FQH states. In chapter 4 we describe a system with a domain wall between the MR and NASS state, both being non-Abelian FQH states. This configuration is obtained by using an auxiliary layer carrying excitations of the minimal model $\mathcal{M}(4,5)$ and tensoring it with the Ising sectors of the MR region. After Bose condensation and confinement of the appropriate fields, this leads to the NASS state. Tab. 4.6 shows the spectra of the excitations that are present in the bulk of the MR and NASS states, as well as the excitations that are strictly confined to the wall between both states. The fusion rules of the wall excitations are of the $\mathbb{Z}_2 \otimes \mathcal{M}(4,5)$ type. Knowing all the fusion rules of the phase diagram we can investigate what kind of processes could occur. For instance, the Majorana fermion can move through the wall from the MR phase into the NASS phase appearing as a ψ_{12} fermion there. Also, dragging a spin-up quasihole from the NASS side through the domain wall results in two types of splitting processes: one where the quasihole splits into two wall excitations and one where it splits into a wall excitation and a quasihole in the MR region. Furthermore, we show how a qubit comprised of two NASS quasiholes can relax its state by exchanging a neutral particle with the boundary, where again it can split into two excitations strictly confined to this boundary.

Chapter 5 presents the results we have obtained by applying symmetry breaking to the hierarchy picture of the FQH states. Several pictures have been proposed in the literature and we have investigated two of these. The HH hierarchy presents states to account for all odd denominator filling fractions in the lowest Landau level. We have induced a phase transition between a state at $\nu = 1/3$ and one at $\nu = 2/5$, where we have found the charges and spins of the excitations in both regions as well as on the boundary between them. The particle with unit electric charge can move between both phases without any interaction with the boundary. Furthermore, the fundamental boundary excitation has charge $e/15$, which agrees with the literature. We also deduce expressions for a system with k general levels of the HH hierarchy. Again, the particle with unit electric charge is able to pass each boundary without leaving a trace. Besides the HH hierarchy, we have investigated the BS hierarchy which aims at describing FQH states in the second Landau level. We concentrated on building the hierarchy on top of the MR state, i.e. building on the state at $\nu = 5/2$. The hierarchization takes place in the $U(1)$ part of the sectors, which enables us to use the results from the HH hierarchy with some small adjustments for the Ising σ sector. First of all, the spectra and quantum numbers of a system with a quantum Hall state at $\nu = 12/5$ built on top of the MR state is obtained. The bulk of the daughter state has two fundamental excitations. Both the spin and elec-

tric charge that we find for these agree with the literature. Moreover, the excitations that can move from the boundary into the bulk of either states are listed in Tab. 5.3. Thus, the other fields are strictly confined to this boundary. The smallest excitation that has to stay on the wall has charge $e/10$. Also, expressions are given of the bulk and boundary spectra for k levels of the BS hierarchy built on top of the MR state.

The deeper one moves into a subject the more questions seem to appear. Therefore, we conclude this thesis by mentioning what remains interesting to consider in future research. For the NASS/MR system we suggest the following two points:

- Since the spectrum we find for the interface between the NASS and MR state differs by a $\mathbb{Z}_2$ factor from the spectrum found in Ref. [36] this should be considered more carefully. For instance, our method does not enable one to directly notice which modes on the interface are gapless and which are gapped. It would be interesting to see if we can manage to distinguish between those modes. Also, we could try to start from a different geometry and see if that reproduces the results of Ref. [36].
- The quantum group breaking only occurred in the non-Abelian part of the MR state. This led to the correct sectors of the NASS state, but we lost the information of the $U(1)$ factors that are possible on the interface between the MR and NASS state. Therefore, it would be interesting to redo the derivation keeping the Abelian part as well. The difficulty in this is that we should start with $\mathcal{M}(4,5)\otimes U(1)$ where we do not know which factors we should choose yet. Most likely, the best way to tackle this problem is by breaking the quantum group $MR\otimes\overline{NASS}$ and see what $U(1)$ factors we get out of this.

The symmetry breaking of a hierarchy of states also has a few open ends:

- Each level of the BS hierarchy has two fundamental excitations, where one contains the trivial sector of the Ising model and the other the σ

sector. Expressions for the charge and spin of the latter remain difficult to find when considering a general level of the BS hierarchy. Therefore, let us sketch where the difficulty lies by first noting how we managed to do it for a specific case. In subsection 5.2.2 we discuss going from the MR state to a phase at $\nu = 12/5$ and for this particular case we do manage to find values of the electric charge for the excitations containing σ. The approach there is to fuse the fundamental excitation $q_1 = (I, 0, 2)$ with itself and see how this product can split into two sectors containing σ. Explicitly this is

$$q_1 \times q_1 = (I, 0, 4) \sim (I, 1, 9) \rightarrow (\sigma, \frac{1}{2}, \frac{9}{2}) \times (\sigma, \frac{1}{2}, \frac{9}{2})$$

Noting that electric charges add under fusion and that q_1 has charge $e/5$, $(\sigma, \frac{1}{2}, \frac{9}{2})$ must also have this charge and is the other fundamental excitation and was denoted by qh_1. Since they generate the spectrum of the first level this enables us to find the electric charges and spins of all the other sectors in the spectrum. For an arbitrary level of the BS hierarchy the difficulty lies in splitting $q_k \times q_k$ into two sectors containing σ, in order to find qh_k.

- So far we have only considered the BS hierarchy where the quasiholes in the 0^{th} level pair up in the trivial fusion channel. It would be interesting to see if we find the same states as in Ref. [47], when the quasiholes pair up in the ψ channel.

- We would like to check if we are able to write down wavefunctions for the states at the different levels of the BS and HH hierarchy. This may be done by taking correlators of vertex operators that insert particles. Since different CFT's can be associated to the same TQFT it is not immediately clear how to do this. Still, we would like to determine how much information is lost when the TQFT is considered instead of the full CFT.

- One of the biggest advantages of the topological symmetry breaking approach is that it naturally gives a description of the edge states in terms of the $\mathcal{T}$-algebra. For the hierarchies we considered everything could be expressed in terms of Wen's K-matrix. We compared our results of the bulk spectra to the results obtained directly from the K-matrix. However, in Ref. [48] it is shown that the K-matrix can also be used to describe the edges of FQH states. Therefore, we would like to compare our results of the edge modes to those of Wen.

- In section 5.1 we mentioned that other hierarchies have been proposed in the literature. Two non-Abelian hierarchies are those of Hermanns in Ref. [43] and Levin and Halperin in Ref. [44]. Both construct

wavefunctions by taking correlators of vertex operators. The former builds a hierarchy by inserting quasiparticles instead of quasiholes. As an explicit example they use the bosonic MR state at $\nu = 4/3$ as the parent state. The higher levels of the hierarchy are all non-Abelian, but the non-Abelian part does differ from the MR state. The latter builds a hierarchy on the fermionic MR state by inserting quasiholes as well as quasiparticles. Remarkably, all the daughter states turn out to be Abelian. It would be a challenge to try to recover their results by applying topological symmetry breaking.

Even though we have successfully applied topological symmetry breaking to several FQH states, much future work remains to be done.

Bibliography

[1] C. Nayak, S.H. Simon, A. Stern, M. Freedman, and S. Das Sarma. Non-Abelian anyons and topological quantum computation. *Rev. Mod. Phys.*, 80:1083, 2008.

[2] J. Preskill. Lecture notes for physics 219: Quantum computation. Chapter 9: Topological quantum computation, 2004.

[3] J. Fuchs. *Affine Lie Algebras and Quantum Groups.* Cambridge University Press, 1992.

[4] F.A. Bais and J.K. Slingerland. Condensate-induced transitions between topologically ordered phases. *Phys. Rev. B*, 79:045316, 2009.

[5] R.E. Prange and S.M. Girvin editors. *The quantum Hall effect.* Springer-Verlag, New York, 1987.

[6] S.M. Girvin. The quantum Hall effect: Novel excitations and broken symmetries. ArXiv:9907002, 1998.

[7] K. von Klitzing, G. Dorda, and M. Pepper. New method for high-accuracy determination of the fine-structure constant based on quantized Hall resistance. *Phys. Rev. Lett.*, 45:494, 1980.

[8] J.P. Eisenstein and H.L. Störmer. The fractional quantum Hall effect. *Science*, 248:1510, 1990.

[9] J.S. Xia, W. Pan, C.L. Vicente, N.S. Sullivan, H.L. Störmer, D.C. Tsui, L.N. Pfeiffer, K.W. Baldwin, and K.W. West. Electron correlation in

the second Landau level: A competition between many nearly degenerate quantum phases. *Phys. Rev. Lett.*, 93:176809, 2004.

[10] D.C. Tsui, H.L. Störmer, and A.C. Gossard. Two-dimensional magnetotransport in the extreme quantum limit. *Phys. Rev. Lett.*, 48:1559, 1982.

[11] R. Willet, J.P. Eisenstein, H.L. Störmer, D.C. Tsui, A.C. Gossard, and J.H. English. Observation of an even-denominator quantum number in the fractional quantum Hall effect. *Phys. Rev. Lett.*, 59:1776, 1987.

[12] W. Pan, J.-S. Xia, V. Shvarts, D.E. Adams, H.L. Störmer, D.C. Tsui L.N. Pfeiffer, K.W. Baldwin, and K.W. West. Exact quantization of the even-denominator fractional quantum Hall states at $\nu = 5/2$ Landau level filling factor. *Phys. Rev. Lett.*, 83:3530, 1999.

[13] R.B. Laughlin. Anomalous quantum Hall effect: an incompressible quantum fluid with fractionally charged excitations. *Phys. Rev. Lett.*, 50:1395, 1983.

[14] F.D.M. Haldane. Fractional quantization of the Hall effect: a hierarchy of incomressible quantum fluid states. *Phys. Rev. Lett.*, 51:605, 1983.

[15] B.I. Halperin. Statistics of quasiparticles and the hierarchy of fractional quantized Hall states. *Phys. Rev. Lett.*, 52:1583, 1984.

[16] J.K. Jain. Composite-fermion approach for the fractional quantum Hall effect. *Phys. Rev. Lett.*, 63:199, 1989.

[17] N. Read and E. Rezayi. Beyond paired quantum Hall state: Parafermions and incompressible states in the first excited Landau level. *Phys. Rev. B*, 59:8084, 1999.

[18] G. Moore and N. Read. Nonabelions in the fractional quantum Hall effect. *Nuclear Physics B*, 360:362, 1991.

[19] L. Saminadayar, D.C. Glattli, Y. Jin, and B. Etienne. Observation of the $e/3$ fractionally charged Laughlin quasiparticle. *Phys. Rev. Lett.*, 79:2526, 1997.

[20] M. Reznikov, R. de Picciotto, T.G. Griffiths, M. Heiblum, and V. Umansky. Observation of quasiparticles with one-fifth of an electron's charge. *Science*, 389:238, 1999.

[21] M. Dolev, M. Heiblum, V. Umansky, A. Stern, and D. Mahalu. Observation of a quarter of an electron at the $\nu = 5/2$ quantum Hall state. *Nature*, 452:829, 2008.

[22] F.E. Camino, W. Zhou, and V.J. Goldman. Realization of a Laughlin quasiparticle interferometer: Observation of fractional statistics. *Phys. Rev. B*, 72:075342, 2005.

[23] C. de C. Chamon, D.E. Freed, S.A. Kivelson, S.L. Sondhi, and X.G. Wen. Two point-contact interferometer for quantum Hall systems. *Phys. Rev. B*, 55:2331, 1997.

[24] P. Bonderson, K. Shtengel, and J.K. Slingerland. Decoherence of anyonic charge in interferometry measurements. *Phys. Rev. Lett.*, 98:070401, 2007.

[25] R. Ilan, E. Grosfeld, K. Schoutens, and A. Stern. Experimental signatures of non-Abelian statistics in clustered quantum Hall states. arXiv: 0803.1542, 2008.

[26] F.E. Camino, W. Zhou, and V.J. Goldman. $e/3$ Laughlin quasiparticle primary-filling $\nu = 1/3$ interferometer. *Phys. Rev. Lett.*, 98:076805, 2007.

[27] N.E. Bonesteel, L. Hormozi, G. Zikos, and S.H. Simon. Braid topologies for quantum computation. *Phys. Rev. Lett.*, 95:140503, 2005.

[28] M.H. Freedman, M.J. Larsen, and Z. Wang. The two-eigenvalue problem and density of Jones representation of braid groups. *Commun. Math. Phys.*, 228:177, 2002.

[29] F.A. Bais, B.J. Schroers, and J.K. Slingerland. Broken quantum symmetry and confinement phases in planar physics. *Phys. Rev. Lett.*, 89:181601, 2002.

[30] F.A. Bais, B.J. Schroers, and J.K. Slingerland. Hopf symmetry breaking and confinement in (2+1)-dimensional gauge theory. *JHEP*, 0305(068), 2003.

[31] C.J.M. Mathy and F.A. Bais. Nematic phases and the breaking of double symmetries. *Ann. Phys.*, 322:709, 2007.

[32] A. Kitaev. Anyons in an exactly solved model and beyond. *Annals of Physics*, 321:2, 2006.

[33] V. Chari and A. Pressley. *A Guide to Quantum Groups.* Cambridge University Press, 1994.

[34] C. Gómez, M. Ruiz-Altaba, and G. Sierra. *Quantum Groups in Two-dimensional Physics.* Cambridge University Press, 1996.

[35] E. Ardonne and K. Schoutens. New class of non-Abelian spin-singlet quantum Hall states. *Phys. Rev. Lett.*, 82:5096, 1999.

[36] E. Grosfeld and K. Schoutens. Non-Abelian anyons: when Ising meets Fibonacci. arXiv: 0810.1955, 2008.

[37] C. Gils, E. Ardonne, S. Trebst, A.W.W. Ludwig, M. Troyer, and Z. Wang. Collective states of interacting anyons, edge states, and the nucleation of topological liquids. ArXiv: 0810.2277, 2008.

[38] F.A. Bais, J.K. Slingerland, and S.M. Haaker. Theory of topological edges and domain walls. *Phys. Rev. Lett.*, 102:220403, 2009.

[39] Ph. Di Francesco, P. Mathieu, and D. Sénéchal. *Conformal Field Theory*. Springer, 1997.

[40] E. Ardonne and K. Schoutens. Wavefunctions for topological quantum registers. *Annals of Physics*, 322:201, 2007.

[41] F.A. Bais, P. Bonderson, S.M. Haaker, and J.K. Slingerland. A quantum group approach to the fractional quantum Hall hierarchy picture. *in preparation*.

[42] P. Bonderson and J.K. Slingerland. Fractional quantum Hall hierarchy and the second Landau level. *Phys. Rev. B*, 78:125323, 2008.

[43] M. Hermanns. Condensing non-Abelian quasiparticles. ArXiv:0906.2073, 2009.

[44] M. Levin and B.I. Halperin. Collective states of non-Abelian quasiparticles in a magnetic field. ArXiv:0812.0381, 2008.

[45] X.G. Wen and A. Zee. Classification of Abelian quantum Hall states and matrix formulation of topological fluids. *Phys. Rev. B*, 46:2290, 1992.

[46] G.A. Fiete, G. Refael, and M.P.A. Fisher. Universal periods in quantum Hall droplets. *Phys. Rev. Lett.*, 99:166805, 2007.

[47] P. Bonderson, A.E. Feiguin, G. Möller, and J.J. Slingerland. Numerical evidence for a $p_x - ip_y$ paired fractional quantum Hall state at $\nu = 12/5$. ArXiv:0901.4965, 2009.

[48] X.G. Wen. Theory of the edge states in fractional quantum Hall effects. *Int. J. Mod. Phys. B*, 6:1711, 1992.

APPENDIX A

Fusion rules MR/NASS interface

In this appendix the fusion rules of the $\mathcal{T}$-algebra corresponding to the MR/NASS interface are shown explicitly in Tab. A.1. We adopt the labeling associated with the NASS and MR sectors. For those sectors that do not belong to either of these theories we use the $\mathcal{M}(4,5)$ labeling. There is one sector that does not fit into the minimal model either so we will just denote this sector by σ^*. There is also a dictionary given in Tab. A.2 that translates between different types of labeling. In this way the initial $\mathcal{A}$ sectors are easily recognized as well as the $\mathbb{Z}_2 \otimes \mathcal{M}(4,5)$ structure of the fusion rules.

	1	σ_3	ρ	ψ	$\tilde{\sigma}'$	$\tilde{\sigma}$	ψ_1	$\sigma_\uparrow$	$\sigma_\downarrow$	ψ_2	σ	σ^*
1	1	σ_3	ρ	ψ	$\tilde{\sigma}'$	$\tilde{\sigma}$	ψ_1	$\sigma_\uparrow$	$\sigma_\downarrow$	ψ_2	σ	σ^*
σ_3		$1+\rho$	$\psi+\sigma_3$	ρ	$\tilde{\sigma}$	$\tilde{\sigma}+\tilde{\sigma}'$	$\sigma_\uparrow$	$\psi_1+\sigma_\downarrow$	$\psi_2+\sigma_\uparrow$	$\sigma_\downarrow$	σ^*	$\sigma+\sigma^*$
ρ			$1+\rho$	σ_3	$\tilde{\sigma}$	$\tilde{\sigma}+\tilde{\sigma}'$	$\sigma_\downarrow$	$\psi_2+\sigma_\uparrow$	$\psi_1+\sigma_\downarrow$	$\sigma_\uparrow$	σ^*	$\sigma+\sigma^*$
ψ				1	$\tilde{\sigma}'$	$\tilde{\sigma}$	ψ_2	$\sigma_\downarrow$	$\sigma_\uparrow$	ψ_1	σ	σ^*
$\tilde{\sigma}'$					$1+\psi$	$\rho+\sigma_3$	σ	σ^*	σ^*	σ	$\psi_1+\psi_2$	$\sigma_\uparrow+\sigma_\downarrow$
$\tilde{\sigma}$						$1+\psi+\rho+\sigma_3$	σ^*	$\sigma+\sigma^*$	$\sigma+\sigma^*$	σ^*	$\sigma_\uparrow+\sigma_\downarrow$	$\psi_1+\psi_2+\sigma_\uparrow+\sigma_\downarrow$
ψ_1							1	σ_3	ρ	ψ	$\tilde{\sigma}'$	$\tilde{\sigma}$
$\sigma_\uparrow$								$1+\rho$	$\psi+\sigma_3$	ρ	$\tilde{\sigma}$	$\tilde{\sigma}+\tilde{\sigma}'$
$\sigma_\downarrow$									$1+\rho$	σ_3	$\tilde{\sigma}$	$\tilde{\sigma}+\tilde{\sigma}'$
ψ_2										1	$\tilde{\sigma}'$	$\tilde{\sigma}$
σ											$1+\psi$	$\rho+\sigma_3$
σ^*												$1+\psi+\rho+\sigma_3$

Table A.1: *Fusion rules of the $\mathcal{T}$-algebra, which describes the interface between a region with Ising sectors and a region with the parafermions of the NASS theory. The colored sectors are confined in the NASS phase. Note that fusing confined sectors (C) and unconfined sectors (UC) has a $\mathbb{Z}_2$ structure: $C \times C = UC$, $C \times UC = C$ and $UC \times UC = UC$.*

1	σ_3	ρ	ψ	$\tilde{\sigma}'$	$\tilde{\sigma}$	ψ_1	$\sigma_\uparrow$	$\sigma_\downarrow$	ψ_2	σ	σ^*
$(1,1)$	$(1,\epsilon)$	$(1,\epsilon')$	$(1,\epsilon'')$	$(1,\tilde{\sigma}')$	$(1,\tilde{\sigma})$	$(\sigma,\tilde{\sigma}')_1$	$(\sigma,\tilde{\sigma})_1$	$(\sigma,\tilde{\sigma})_2$	$(\sigma,\tilde{\sigma}')_2$	$(\sigma,1)$	(σ,ϵ)
$(1,1)$	$(1,\epsilon)$	$(1,\epsilon')$	$(1,\epsilon'')$	$(1,\tilde{\sigma}')$	$(1,\tilde{\sigma})$	$(-1,1)$	$(-1,\epsilon)$	$(-1,\epsilon')$	$(-1,\epsilon'')$	$(-1,\tilde{\sigma}')$	$(-1,\tilde{\sigma})$

Table A.2: *Relabeling the sectors can be useful. The top row gives the labeling as used in Tab. A.1. The second row translates to a labeling in terms of the initial $\mathcal{A}$-algebra, where we have chosen a representatives of the fields that became identified with each other in the broken phase. Upon fusion with (ψ, ϵ'') the other $\mathcal{A}$ sectors can be found. The last line shows the $\mathbb{Z}_2 \otimes \mathcal{M}(4,5)$ structure of these fusion rules explicitly.*

Dankwoord

Deze twee laatste pagina's wil ik gebruiken om stil te staan bij al die mensen die belangrijk voor mij zijn geweest, tijdens het afgelopen jaar waarin ik dit afstudeer onderzoek heb gedaan en het allemaal op papier heb gezet.

In de eerste plaats wil ik degene bedanken die hier de grootste rol in heeft gespeeld. Sander, ik had me geen betere begeleider kunnen voorstellen. Het onderwerp dat je me aanreikte heeft me gegrepen en daar ben ik je dankbaar voor. Naast het resultaat van de scriptie zelf, heb je me nauw begeleid in de wereld van het onderzoek en je enthousiasme werkte aanstekelijk. Met een publicatie op zak en hopelijk een tweede in aantocht kan ik mij geen betere start voor de komende vier jaar wensen. Daarnaast waren je interesse in mij als persoon en de vele chitchat momenten die we hebben gehad, een welkome afwisseling op het serieuzere werk.

Joost Slingerland wil ik bedanken voor de prettige samenwerking. Elke vraag die ik over het onderwerp had wist je feilloos en met veel geduld uit te leggen. Kareljan Schoutens heeft de tijd voor mij genomen om mijn vragen over de NASS toestand en qubit relaxatie te beantwoorden. Hier ben ik je dankbaar voor en ik kijk uit naar de samenwerking tijdens mijn promotie onderzoek de komende vier jaar.

De taak van het proeflezen van mijn scriptie hebben twee "leken" op zich genomen. Gijs en mama, wat een doorzettingsvermogen heeft dit van jullie gevraagd. Met diep medelijden zag ik toe hoe jullie je door deze tekst hebben heen gewerkt om het taalgebruik te verbeteren. Dit is mijn scriptie absoluut ten goede gekomen.

I would also like to thank a few of my fellow students: Evert, Wolf, Sebas, Lucas, Giota, Milosz and Dimitrios for being in the same situation. I enjoyed

sharing a hall with you and having lunch and lots of coffee. Daarnaast wil ik ook nog Olaf en Balt noemen. Olaf bedankt voor het beantwoorden van alle vragen over het quantum Hall effect die ik had, tijdens mijn eerste maanden van het onderzoek. Hopelijk komen er veel conferenties die we samen zullen bezoeken de komende jaren. Balt, bedankt voor de ondersteuning op het gebied van computers.

Dan is er nog een aantal mensen dat ik wil bedanken dat niet direct iets met mijn studie te maken had, maar toch een bijdrage heeft geleverd het afgelopen jaar. Nens, Lies en Maaike, jullie hebben de lunches bij de Sorbon naar een hoger plan getild. De vele broodjes ei smaakten een stuk beter in jullie aanwezigheid. Ook de koffie in de Kriterion, Krater en zelfs de Mensa smaakte vurrukkulluk!

Mijn familie wil ik bedanken voor het geduld in mij. Het begrip voor mijn fysieke afwezigheid, maar als ik er wel was soms ook mentale afwezigheid, was eindeloos en zeer belangrijk voor mij, omdat ik me er wel degelijk druk om maakte. Speciaal wil ik hier mijn oudste zus Gallieth noemen. Bedankt voor de vele keren dat je voor me gekookt hebt of gewoon even langs kwam.

De allerlaatste woorden van deze scriptie wijd ik aan mijn vriend Gijs. Het is één groot feest om met jou samen te zijn!